

Non-Baryonic Dark Matter: Observational Evidence and Detection Methods

Lars Bergström

Department of Physics, Stockholm University, Box 6730, SE-113 85 Stockholm,
Sweden, lbe@physto.se

Abstract. The evidence for the existence of dark matter in the universe is reviewed. A general picture emerges, where both baryonic and non-baryonic dark matter is needed to explain current observations. In particular, a wealth of observational information points to the existence of a non-baryonic component, contributing between around 20 and 40 percent of the critical mass density needed to make the universe geometrically flat on large scales. In addition, an even larger contribution from vacuum energy (or cosmological constant) is indicated by recent observations. To the theoretically favoured particle candidates for non-baryonic dark matter belong axions, supersymmetric particles, and of less importance, massive neutrinos. The theoretical foundation and experimental situation for each of these is reviewed. Direct and indirect methods for detection of supersymmetric dark matter are described in some detail. Present experiments are just reaching the required sensitivity to discover or rule out some of these candidates, and major improvements are planned over the coming years.

PACS numbers: 12.60.Jv, 12.90.+b, 14.80.Ly, 14.80.Mz, 95.30.Cq, 95.35.+d, 97.20.Vs, 98.35.Gi, 98.62.Gq, 98.80.Cq, 98.80.Es, 98.80.Ft

Submitted to: *Rep. Prog. Phys.*

1. Introduction

During the past few years, remarkable progress has been made in cosmology, both observational and theoretical. One of the outcomes of these rapid developments is the increased confidence that most of the energy density of the observable universe is of an unusual form, i.e., not made up of the ordinary matter (baryons and electrons) that we see around us in our everyday world.

The only realistic model for cosmology, and one that has become more solidly established by recent observations, is the big bang model. According to this Standard Model of cosmology, the universe has been and still is expanding from a compressed and hot phase, which existed some 15 billion years ago. The observational cornerstones of the big bang model – the expansion of the universe, the fossil record of light elements synthesized during the first few minutes, and the existence still today of an intense thermal radiation field, the cosmic microwave background – created when neutral atoms formed around 300 000 years after the big bang – are more solid than ever. In fact, cosmology is entering an era of precision measurements, when information from all these three important processes is becoming accurate enough that it can be used to clarify the detailed structure and evolution of our Universe.

For example, big bang nucleosynthesis can be used to determine the baryon fraction of the matter density in the universe quite accurately [1], and combined with analyses of galaxy cluster dynamics, supernova data and the cosmic microwave background radiation this gives convincing arguments for the existence of a large amount of non-luminous, i.e., dark, matter. The matter content of the universe seems to be at least a factor of 5 higher than the maximum amount of baryonic matter implied by big bang nucleosynthesis. This dark matter is thus highly likely to be “exotic”, i.e, non-baryonic [2].

There are also indications, although still somewhat preliminary, of the existence of vacuum energy, corresponding to the famous “cosmological constant” that Einstein introduced but later rejected (although without very good reasons) in his theory of general relativity. An alternative possibility is a slowly varying scalar field, “quintessence” [3] which, like vacuum energy, does not cluster at all (or on very large scales only). This possibility has recently been given increased attention due to results from Type Ia supernova surveys [4, 5] as will be discussed later in this review.

Although the existence of non-baryonic dark matter is now generally accepted by most of the astrophysical community, the nature of the dark matter is one of the outstanding questions in standard cosmology [6]. In fact, since 1998 there is for the first time strong evidence for the existence of non-baryonic dark matter in the universe, in the form of massive neutrinos. This is due to the discovery of atmospheric neutrino oscillations in the Super-Kamiokande experiment [7]. However, the natural neutrino mass scale of around 0.1 eV which is implied by the neutrino oscillation data is not large enough to influence cosmology in a dramatic way (although this type of non-baryonic dark matter would contribute about as much to the total mass density of the

universe as do the visible stars).

Even if the mass of one of the neutrinos is higher (up to, say, 5 eV which would be possible if neutrinos are nearly degenerate in mass or if there exist a fourth, sterile neutrino), the mass density would not be large enough to explain the matter fraction of the cosmic average density. There are also arguments from galactic structure against an all-neutrino dark matter population. Therefore, it is natural to ask which other fundamental particles could be good dark matter candidates.

This review is organized as follows. In Section 2 the general framework of modern cosmology is briefly reviewed. In Section 3 the fundamental mechanism of thermal production of relic particles in the early universe is explained. In Section 4 various estimation methods for the amount of different forms of mass and energy density on several length scales in the universe are discussed. In Section 5 the possible contribution from hidden ordinary matter (baryons) is treated, and the evidence for a population of dark baryonic objects, “MACHO”s (MAssive Compact Halo Objects), displayed. The distribution of dark matter in galaxies, in particular the in Milky Way which most of the detection experiments are sensitive to, is discussed in Section 6. Particle physics models for non-baryonic dark matter are treated in Section 7, and the presently most discussed models for Weakly Interacting Massive Particles (“WIMP”s), namely the supersymmetric models, are reviewed in Section 8. These models, which have been developed in detail in the current literature, also serve as useful templates for other, yet unthought of, particle models for dark matter. Therefore, Section 9 deals mainly with the methods of detection of the lightest electrically neutral supersymmetric particle, the neutralino, which is a quantum mechanical mixture of the supersymmetric partners of the photon, the Z^0 boson and the neutral scalar Higgs particles. Section 10 ends the review with some concluding remarks and an outlook.

2. Basics of standard cosmology

The big bang model has its theoretical base in Einstein’s general theory of relativity, which has been thoroughly tested on many different length scales, and which so far has agreed with all observations.

The fundamental dynamical degrees of freedom of the gravitational field are the components of the metric tensor, which enter into the line element describing the distances between nearby points in space-time. To make cosmology tractable, one has to assume that the universe is isotropic and homogeneous on the average. This agrees, of course, with observations. On the largest scales probed by the cosmic microwave background, the observed temperature anisotropies, which are related to the density fluctuations at the time of emission, are smaller than one part in 10^4 . (There is a dipole component which is of the order of 10^{-3} , but this is interpreted as being of kinematical origin, caused by our motion with respect to the local cosmic rest frame.)

One can show that every isotropic, homogeneous three-space can be parametrized, perhaps after performing a coordinate transformation, by coordinates which give a line

element, squared distance between points at a fixed time, of the form

$$ds^2 = a^2 \left(\frac{dr^2}{1 - kr^2} + r^2 d\Omega^2 \right), \quad (1)$$

where the constant k after a suitable normalization of r can take one of the three values $k = -1, 0, +1$, depending on whether the geometry is open, flat or closed. For a given value of k , this defines a one-parameter family of similar spaces, where the scale factor a is the parameter. These are the Friedmann-Lemaitre-Robertson-Walker (FLRW) models. For the simplest case $k = 0$, we see that the metric describes ordinary Euclidean three-space with the scale factor a giving the overall normalization of physical distances. Due to the observed expansion of the universe, we know that the scale factor depends on time, $a = a(t)$ with $\dot{a}/a > 0$ at the present time $t = t_0$, and a basic task for standard cosmology is to determine k and to compute $a(t)$, both in the past and in the future.

2.1. The Friedmann equation

The time dependence of the scale factor a is given by the Friedmann equation (which follows from one of the components of Einstein's tensor equations):

$$\left(\frac{\dot{a}}{a} \right)^2 + \frac{k}{a^2} = \frac{8\pi G_N}{3} \rho_{tot}, \quad (2)$$

where G_N is Newton's gravitation constant, and ρ_{tot} is the total average energy density of the universe. The latter gets contributions at least from matter, radiation and perhaps vacuum energy (cosmological constant),

$$\rho_{tot} = \rho_m + \rho_r + \rho_\lambda. \quad (3)$$

In particle physics units, $\hbar = c = 1$, (which means that all dimensionful quantities can be expressed in powers of some mass unit, e.g., 1 GeV), G_N has the dimension of the inverse of a squared mass, the Planck mass, which has the huge value of $1.22 \cdot 10^{19}$ GeV. From the particle physics viewpoint, this means that gravity is governed by some still unknown theory at superhigh energy, whose low-energy limit is Einstein's general theory of relativity. The prime candidate for such a fundamental theory is string theory or one of its related versions, but this is an active, on-going field of research.

The overall value of the scale factor is arbitrary, only relative changes are measurable. The Hubble parameter (which depends on time) is

$$H(t) = \frac{\dot{a}(t)}{a(t)} \quad (4)$$

and governs the local expansion according to Hubble's law, $v = Hd$, where v is the recession velocity and d is the physical distance. Observationally, the present value H_0 of the Hubble parameter (called the Hubble constant) is uncertain to around 20 %, and one usually writes

$$H_0 = h \cdot 100 \text{ km s}^{-1} \text{ Mpc}^{-1} \quad (5)$$

with $h = 0.65 \pm 0.15$ encompassing most recent observational determinations of the Hubble constant (1 Mpc is approximately $3.1 \cdot 10^{22}$ m). In SI units,

$$H_0 = 3.2 \cdot 10^{-18} h \text{ s}^{-1}. \quad (6)$$

Consequently, the linear length scale of the universe is presently being stretched by a fraction of $3.2 \cdot 10^{-18} h$ per second. The inverse of this expansion rate defines a time, the Hubble time $t_H = 9.8 h^{-1}$ years. In standard cosmology, the present age of the universe is of this order of magnitude modulo a numerical factor slightly less than unity reflecting the fact that the expansion rate most of the time should have been larger than today. In particle physics units ($\hbar = c = 1$) the expansion rate has the dimension of mass, the numerical value being $2.1 \cdot 10^{-42} h$ GeV. The large value of the Planck mass compared to the expansion mass scale (and all other other fundamental mass scales in nature) is one of the unsolved problems of theoretical physics.

We see from Eq. (2) that the universe is flat ($k = 0$) when the energy density equals the *critical density* ρ_c , given by

$$\rho_c \equiv \frac{3H^2}{8\pi G_N}. \quad (7)$$

From Eq. (5), its present numerical value is computed to be $\rho_c^0 = 1.9 \cdot 10^{-38} h^2 \text{ kg m}^{-3}$. The Friedmann equation (2) can then be written in the equivalent form

$$\frac{k}{H^2 a^2} + 1 = \frac{\rho}{\left(\frac{3H^2}{8\pi G_N}\right)} \equiv \Omega, \quad (8)$$

where

$$\Omega \equiv \frac{\rho}{\rho_c} \quad (9)$$

or

$$\frac{k}{H^2 a^2} = \Omega - 1. \quad (10)$$

We thus see that Ω is the energy density in units of the critical density, and $\Omega = 1$ is equivalent to having a flat universe ($k = 0$).

The expansion of the universe means that the scale factor $a(t)$ has been increasing since the earliest times after the big bang. The first observational evidence for this was of course Hubble's detection of a cosmological redshift of the light emitted by distant galaxies. For an emitted wavelength (e.g., associated with a specific spectral line) λ_{emit} and an observed wavelength λ_{obs} the redshift parameter z is defined by

$$1 + z \equiv \frac{\lambda_{obs}}{\lambda_{emit}}. \quad (11)$$

In the standard FLRW model of cosmology, the redshift is related to the change in scale factor $a(t)$ through the relation (see [6] for a simple derivation)

$$1 + z = \frac{a(t_{obs})}{a(t_{emit})}. \quad (12)$$

3. Creation of relic particles

In a universe which expands, there is at each epoch a mixture of different particles in thermal contact with each other, maintaining a temperature which evolves with time. For instance, when the temperature of the universe was much larger than a few MeV, electromagnetic interactions kept electrons and positrons in thermal equilibrium and weak interactions kept also neutrinos in equilibrium. However, to maintain this equilibrium, interactions had to be frequent enough. The critical time scale is set by the Hubble parameter, which has the dimensions of 1/time. The interaction rate per particle with velocity v is given by $\Gamma = n\sigma v$, where n is the number density of “target” particles and σ is the cross section[‡]. Choosing units such that $\hbar = c = k_B = 1$ (i.e., also the temperature is measured in mass units), the thermal equilibrium number density for a particle species of mass m_i is, at temperature T

$$n_i = \frac{g_i}{(2\pi)^3} \int f_i(\mathbf{p}) d^3\mathbf{p}, \tag{13}$$

with

$$f_i(\mathbf{p}) = \frac{1}{e^{\frac{E_i}{T}} \pm 1}, \tag{14}$$

where $E_i = \sqrt{\mathbf{p}^2 + m_i^2}$ is the energy and the plus sign applies for fermions which obey Fermi-Dirac statistics, the minus sign for bosons (Bose-Einstein statistics). In the non-relativistic limit $T \ll m_i$, the integral can be solved, and one obtains the familiar result

$$n_{NR} = g_i \left(\frac{m_i T}{2\pi} \right)^{3/2} e^{-m_i/T} \tag{15}$$

which shows the exponential suppression of heavy particles expected due to the relativistic rest energy $E_i^0 = m_i$. The degeneracy parameter g_i counts the independent degrees of freedom (i.e. the number of helicity states). For photons, $m_\gamma = 0$, $g_\gamma = 2$. For neutrinos, m_ν is unknown but presumably very small, with a total of $g_\nu = 6$ (three neutrinos of negative helicity and three antineutrinos of positive helicity – the other helicity states are missing reflecting the maximal parity violation of the weak interactions). In the other solvable regime, the relativistic one ($T \gg m_i$), the rest energy of particles can be neglected, and the number density becomes

$$n_R = s_i g_i \frac{\zeta(3) T^3}{\pi^2} \tag{16}$$

where $s_i = 1$ for bosons and $s_i = 3/4$ for fermions.

The important point to notice is the absence of any exponential suppression, which means that at a given epoch the number density of relativistic particles by far outweighs that of nonrelativistic particles, as long as thermal equilibrium is maintained.

[‡] In a more refined treatment, one has to solve the Boltzmann transport equation, which couples all different particle species, in a background metric given by the FLRW model. This also allows to follow the deviations from exact thermal equilibrium caused by the expansion. The results of our simplified discussion are in rough agreement with this treatment.

The corresponding energy densities are also easily obtained by inserting a factor E_i in the integrand of Eq. (13). Again, nonrelativistic particles contribute a negligible amount, and for relativistic particles the result is

$$\rho_R = u_i g_i \left(\frac{\pi^2 T^4}{30} \right) \quad (17)$$

with $u_i = 1$ for bosons and $u_i = 7/8$ for fermions.

The Friedmann equation (2) now shows that the expansion rate H evolves as

$$H^2 = \frac{8\pi G_N}{3} \frac{\pi^2 T^4}{30} \sum_i g_i u_i, \quad (18)$$

where the small terms from curvature and non-relativistic particles have been neglected.

We are now in a position to compute the temperature at which neutrinos decoupled in the early universe. The cross section for neutrinos is of weak interaction strength meaning $\sigma \propto G_F^2 s$ with G_F the Fermi coupling constant $\sim 1/m_W^2$, and s the total energy squared in the centre of mass, i.e., $s \propto T^2$ for relativistic particle collisions. For thermal equilibrium to be maintained, one has to demand that each particle has interacted at least once during a Hubble time $\sim H^{-1}$. Comparing thus the expansion rate H with $n\sigma v$ (using that $n \propto T^3$ and v is of order unity), neglecting the constant numerical factors, a simple calculation shows that at a temperature of around 3 to 4 MeV the interaction rate fell below the expansion rate. After that, neutrinos would have a fixed comoving number density and a distribution that would look like thermal, but the energies of neutrinos, while still relativistic, would redshift with the expansion similarly to the photons of the microwave background radiation. A more careful evaluation, keeping all numerical factors, gives as a result that the “neutrino background” which should exist in the universe, now has a number density of around 50 cm^{-3} neutrinos per degree of freedom (i.e. of the order of 300 cm^{-3} in total).

We now see an important possibility, which was historically the first serious attempt to explain the dark matter problem using particle physics. If neutrinos have a finite but small mass, they should have the number density just computed, but since the effective temperature due to the expansion may be lower than the neutrino mass they would be non-relativistic at the present epoch and contribute significantly to the energy density of the universe. Quantitatively, one obtains

$$\Omega_\nu h^2 = \frac{\sum_i m_{\nu_i}}{93 \text{ eV}}. \quad (19)$$

If the particle is more massive, so that it is non-relativistic at decoupling, the mathematical treatment is a little more involved (since the exact form of Eq. (13) has to be used when tracking the interaction and expansion rates, and also the cross section will be a more complicated function of temperature), but identical in principle. A general framework for obtaining a numerical solution, even in the presence of resonances and particle production thresholds in the expression for the cross section, can be found in [8], and a simple treatment in [9]. As a first-order estimate, the contribution to Ω_M from

a massive particle χ depends only on its annihilation cross section σ_A and not explicitly on its mass (to logarithmic accuracy). The resulting Ω_χ is then [10]

$$\Omega_\chi h^2 \sim \frac{3 \cdot 10^{-27} \text{ cm}^3 \text{ s}^{-1}}{\langle \sigma_A v \rangle} \quad (20)$$

where $\langle \dots \rangle$ indicates taking a thermal average. Usually, $\sigma_A v$ is dominated by S wave processes, and then it is nearly velocity-independent and therefore temperature-independent. If the S wave is forbidden by selection rules, or if there exist particle poles or thresholds in or near the physical region for the process, the temperature corrections can be large. An interesting consequence of the result in Eq. (20) is that massive particles which have interactions of the order of the weak interactions naturally give contributions to Ω_M of order unity. The generic name for such a dark matter candidate is a WIMP (Weakly Interacting Massive Particle). For massive particles (heavier than a few GeV), the freeze-out temperature (the temperature at which the number density of the particle leaves the thermal equilibrium curve) is typically 4 to 5 % of the particle mass, i.e., they are non-relativistic already at the decoupling epoch.

Although thermal production of stable particles is a generic, unavoidable mechanism in the big bang scenario, there are several additional processes possible. For instance, some very heavy particles were perhaps never in thermal equilibrium. Non-thermal production may also occur near cosmic strings and other defects as happens, for instance, in the case of axions discussed in Section 7.5. Near the end of a period of early inflation, several mechanisms related either to the inflaton field or to the strong gravity present at that epoch could contribute to nonthermal production (see, e.g., [11]).

4. The Amount of Matter and Energy in the Universe

The big bang model contains a strong implicit connection between particle physics and cosmology. In the early universe, the thermal energies were high enough that even the heaviest of the known particles could be pair created and destroyed in near-equilibrium processes. As time evolved, the universe may have gone through a whole series of phase transitions, e.g., the electroweak transition when the W and Z bosons got their mass, and the confinement transition from a quark-gluon plasma to bound quark (and antiquark) states.

4.1. Inflation

The particle physics – cosmology connection became much stronger in the beginning of the 1980s with the discovery of the cosmological inflation mechanism [12]. Traditional big bang cosmology suffers from problems concerning initial conditions. For instance, why is it that the microwave background radiation has nearly the same temperature even in oppositely directed regions on the sky which cannot have been in causal contact at the time of emission? This is sometimes called the horizon problem. Inflation solves this by assuming that some scalar “inflaton” field in the early universe slowly changed

its expectation value due to a temperature-dependent effective potential which left the field temporarily at a non-minimum. If the potential energy density during this “slow-roll” phase was almost constant, and dominated the energy density of the universe at that time, it acted in a similar way as a true cosmological constant. This would cause according to Eq. (2) a constant value of the Hubble parameter H , and the equation

$$\left(\frac{\dot{a}}{a}\right)^2 = H^2 = \text{const} \tag{21}$$

is easily solved to give

$$a(t) \propto e^{Ht} \tag{22}$$

which means a superluminal (exponential) expansion[§]. This enormously rapid expansion implied that regions that had been in causal contact moved outside the horizon of each other. The inflationary epoch stopped when the scalar field had rolled down to the true minimum of the potential. Due to the energy released by damped, coherent oscillations of the field around this minimum the universe was refilled with particles and radiation and an enormous amount of entropy was created (the reheating epoch). After this, the universe restarted in something similar to the traditional big bang cosmology, but with very smooth and flat initial conditions.

In particular, a generic prediction from inflation is thus that the universe is very close to flat, i.e., $k = 0$. Then $\Omega_{\text{tot}} = \Omega_0 = 1$, with the subscript 0 referring to the value at the present time $t = t_0$, $\Omega_0 \equiv \Omega_{\text{tot}}(t_0)$.

Inflation is strictly speaking not a mandatory ingredient in the modern Standard Model of cosmology, but in lack of alternative explanations of, e.g., the horizon problem it has a prominent place in theoretical cosmology. An additional virtue of inflation is that it gives a possible explanation of the origin of the small primordial fluctuations seen in the microwave background. This could be caused by vacuum fluctuations of the inflaton field, which are expected in most models of inflation to be gaussian and nearly scale-invariant. As more accurate measurements of the cosmic microwave background are soon to be expected (see Section 4.5), these features will be tested further.

4.2. Different forms of energy density

In general, if $\Omega \neq 1$ it is time-dependent, see Eq. (10). Even if $\Omega_0 = 1$ as predicted by inflation, the various different contributions to $\Omega_{\text{tot}}(t)$ depend differently on time, and therefore on redshift. It is thus important to determine how the total energy density in the universe is divided into its main components $\Omega_M = \Omega_B + \Omega_{DM}$ and Ω_Λ , with $\Omega_0 = \Omega_M + \Omega_\Lambda$. Here we have separated the mass contribution into a baryonic part Ω_B and a non-baryonic, dark-matter part Ω_{DM} . We take the capital subscripts to refer to present-day values, i.e., $\Omega_M = \Omega_m(t_0)$ etc. From Eq. (10) it can be seen that an eventual

[§] This is in no contradiction with relativity, since it is space itself which expands. Locally, in any given small region, matter has to move with a velocity less than the velocity of light.

deviation from $\Omega_0 = 1$ can be interpreted as a present-day contribution from curvature to the expansion rate. Sometimes, one therefore introduces

$$\Omega_K = \frac{-k}{a_0^2 H_0^2} \tag{23}$$

in which case a sum rule is obtained:

$$\Omega_M + \Omega_\Lambda + \Omega_K = 1. \tag{24}$$

This makes the three Ω variables similar to the so-called Dalitz variables in particle physics, and the various portions of this parameter space allowed or disfavoured by measurements may be displayed in triangular “Dalitz plots” (see, e.g., [2]).

Even if $\Omega_0 = \Omega_M + \Omega_\Lambda = 1$, the relative weights of the various contributions generally depend on time and therefore on redshift z . In particular, the matter density scales as $(1+z)^3$ since a constant comoving number density causes the physical mass density to be diluted with the changing volume, whereas the cosmological constant is simply constant. This means that

$$\frac{\Omega_\lambda}{\Omega_m} = \frac{\Omega_\Lambda}{\Omega_M (1+z)^3} \tag{25}$$

so that the cosmological constant was insignificant at early times (high z), but will eventually dominate the total density. At redshifts higher than 1000, also radiation, scaling as $(1+z)^4$ was important, but can be safely neglected in today’s universe, since measurements of the flux of cosmic background radiation photons which dominate the radiation energy density give $\Omega_R \sim 10^{-5} - 10^{-4}$. Of course, there could in principle also exist other forms of energy. If an equation of state relating the energy density and the pressure of component X , $\rho_X = \alpha_X p_X$ is valid, then Ω_X scales with z as $(1+z)^{3(1+\alpha_X)}$. Vacuum energy, or equivalently a cosmological constant, can then be seen as a special case with $\alpha_\Lambda = -1$. A general expression for the expansion rate is [6]

$$\begin{aligned} \frac{H^2(z)}{H_0^2} = & \left[\Omega_X (1+z)^{3(1+\alpha_X)} + \Omega_K (1+z)^2 \right. \\ & \left. + \Omega_M (1+z)^3 + \Omega_R (1+z)^4 \right]. \end{aligned} \tag{26}$$

The different dependence on z is the key to disentangling all the possible contributions to Ω_0 , by observations at different, and preferably large, redshifts. Also, as we will see, planned precision measurements of the cosmic microwave background radiation may be very helpful in determining all these parameters, as well as several other presently ill-determined cosmological parameters.

4.3. *Supernova cosmology*

Until a couple of years ago, the theoretically favoured FLRW model was the Einstein – de Sitter model which has $\Omega_M = 1$, $\Omega_\Lambda = 0$. The justification for this model is that it is compatible with inflation, and avoids the severe finetuning problem of having a cosmological constant Λ which is non-zero but still some 120 orders of magnitude smaller

than inferred from the natural energy scale of quantum gravity, $\Lambda \sim m_{\text{Pl}}^4$ [13, 14]. It is, however, impossible to quantify how severe this finetuning is since there exists at present no established theory of quantum gravity. Also, most dynamical estimates of Ω_M on galaxy and cluster scales have consistently given much smaller values of $\Omega_M \sim 0.2 - 0.4$ [15].

Since agreement between observations and the big bang nucleosynthesis (BBN) prediction of helium, lithium and deuterium abundance and puts an upper limit to the baryonic contribution Ω_B of [1]

$$\Omega_B h^2 \leq 0.019, \tag{27}$$

non-baryonic dark matter has to dominate the energy density by a large factor, even if Ω_M would be as low as 0.3. Also, we will see that there are other problems with an all-baryon universe especially as concerns the formation of structure.

A recent shift of most favoured cosmological model has occurred thanks to the new determinations of the geometry of the universe using Type Ia supernovae as standard candles. The idea is simply that the line element in Eq. (1) implies a different ratio of angular diameter to radial distance for the different values of k . Moreover, since the finite propagation speed of light means that one probes an earlier epoch of the universe when making observations at large redshifts, the different z -dependence of the various contributions to Ω will influence the relation between observed luminosity and the redshift (see Eq. (26)). This new type of analysis of the energy contents of the universe seems to require a non-vanishing Ω_Λ [2], especially when combining the supernova data with data from the cosmic microwave background (CMB) radiation [16]. The presently “best-fit” cosmological model which is compatible with $\Omega_0 = 1$ has $\Omega_M \sim 0.3 \pm 0.2$, $\Omega_\Lambda \sim 0.7 \mp 0.2$, where the error estimates are indicative only. Relaxing the requirement $\Omega_0 = 1$ gives a larger, cigar-shaped region in the Ω_M - Ω_Λ plane (see Fig. 1), but data from both groups [4, 5] support a non-zero Ω_Λ at the level of two or three standard deviations. Fixing $\Omega_0 = 1$, as predicted by inflation and as seems preferred by the cosmic microwave background data discussed in Section 4.5, the mentioned values $\Omega_\Lambda \sim 0.7 \pm 0.2$, $\Omega_M \sim 0.3 \mp 0.2$ emerge.

This is a field of great potential which evolves rapidly, and the use of the infrared camera on the Hubble Space Telescope should make follow-up observations of high- z objects easier. Eventually, a dedicated satellite would allow more than an order of magnitude improvement of the statistics with an accompanying hope of a better understanding the sources of systematic errors, for instance evolution of metallicity of the progenitor stars and the effects of absorption of grey dust.

4.4. Gravitational lensing

According to the predictions of Einstein’s general relativity, the curvature of space-time caused by matter gives rise to a deflection of light rays, something first verified by Eddington in 1919. Since the deflection angle is proportional to the mass of the object causing the deflection (the “lens”), one has in principle a good tool for estimating

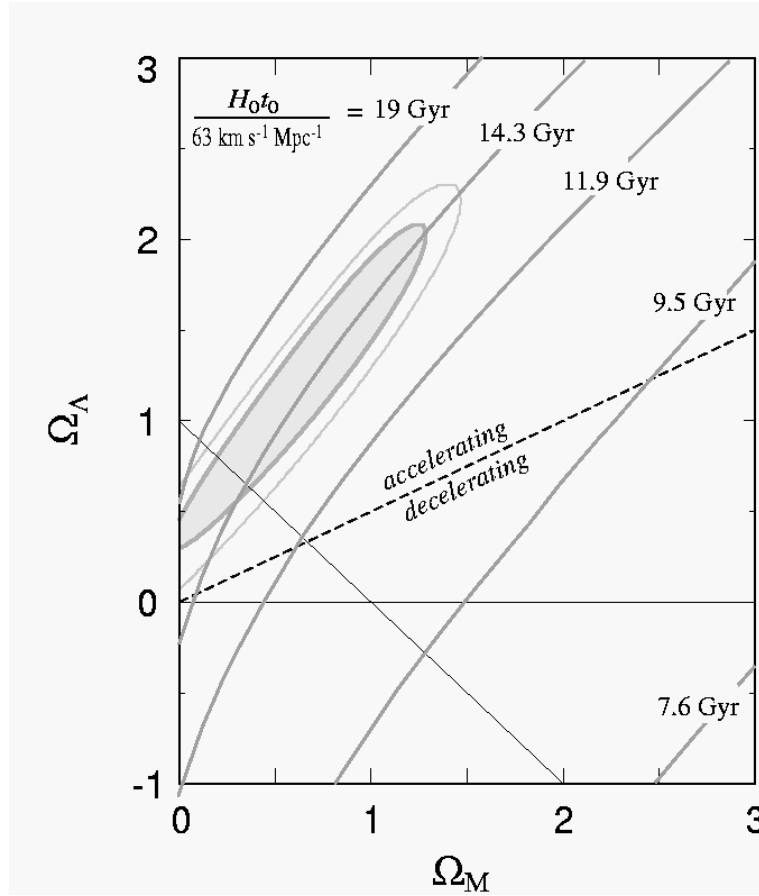


Figure 1. Best-fit coincidence regions in the Ω_M - Ω_Λ plane from the analysis of the *Supernova Cosmology Project* [4]. The dark and light ellipses show the 68 per cent and 90 per cent confidence regions. A flat Universe ($\Omega_K = 0$) would fall on top of the diagonal solid line passing through the prediction from inflation $\Omega_0 = \Omega_M + \Omega_\Lambda = 1$. To the right of that line the Universe is closed, and to the left it is open. The dashed line shows the division between acceleration and deceleration for the Universe. Also shown are isochrones of constant age. Figure kindly provided by A. Goobar, The Supernova Cosmology Project [4].

directly the mass of astrophysical objects, from planets and upwards to galaxies and galaxy clusters. In the latter case, distant bright galaxies and galaxy nuclei such as quasars are very useful as sources. Usually they can be considered as being pointlike, and an excellent signature of gravitational lensing is the appearance of multiple images of one and the same quasar. The masses of the lensing objects determine the angular separation of images, and the frequency of lensing events has a strong dependence on the geometry of the universe, in particular the presence of vacuum energy [17, 18].

The gravitational lensing analysis of [19], based on the frequency of double images in large surveys of quasars indicates that there is plenty of dark matter; the 95 % c.l. limits are $\Omega_M > 0.38$ and $\Omega_\Lambda < 0.66$. An analysis of the number of arcs from gravitational lensing of clusters expected in various cosmologies on the other hand gives

consistency for an open model with $\Omega \sim 0.3 - 0.4$, but failure for closed models with or without a cosmological constant [20]. This consequently may be marginally in conflict with the supernova results. However, gravitational lensing has its own problems with systematic errors related to selection effects and uncertainties in the lens models. That individual galaxies and galaxy clusters are completely dominated by dark matter with the visible baryonic matter being subdominant is, however, demonstrated without doubt in analyses of strong lensing of background galaxies [21].

There is hope that future more complete surveys of gravitational lenses, also the lensing of supernovas, may give information on whether the dark matter is distributed in the form of compact massive objects or in more diffuse form [22, 23, 24].

Although the analyses mentioned so far seem to point to a matter density smaller than critical, one should not disregard the possibility that the simple Einstein – de Sitter model could be correct. For instance, the supernova data may be plagued by larger than anticipated systematical errors. Also, there exist indications for a large value of Ω_M and a small Ω_Λ on the very largest scales [25].

A problem for high- Ω_M models without cosmological constant was until very recently the difficulty of reconciling the age of the universe t_U based on the present expansion rate H_0 with the estimated age of the oldest globular clusters. The values $\Omega_M = 1$, $\Omega_\Lambda = 0$ give $t_U = 2/(3H_0)$, which for $h = 0.6$ implies $t_U \sim 10 - 11$ Gyr. The determination of globular cluster ages on the other hand used to give 14 – 15 Gyr as best estimates. Besides some doubts that may still remain about the accuracy of these latter very indirect means of bounding the age of the universe, the recalibration of the distance scale provided by the Hipparcos satellite parallax measurements has brought the globular cluster age limit down by 2-3 Gyr [26], with the one-sided 95 % c.l. lower limit being 9.5 Gyr. This means that a critical universe is now marginally allowed without a cosmological constant, if $h \lesssim 0.6$, a value that is not far from the current best estimates. The presence of a cosmological constant generally increases the age for a given value of the Hubble constant, so the “age problem” is not regarded as very severe anymore.

At present the emerging, but cautious, consensus is that a non-zero cosmological constant may be needed. This recent paradigm shift is mainly driven by the outcome of new observations. Still there are severe theoretical problems related to the smallness of the required cosmological constant expressed in natural particle physics units. One cause of vacuum energy according to field theoretical models is the expectation value of various scalar field potentials. Since the mass scale of these vacuum expectation values should be of the order of the mass scale of the physics involved, a phenomenal cancellation between several sources of has to occur, since the sub-eV value needed is many orders of magnitude below any known phase transition (electroweak, QCD, supersymmetric. . .) that could be relevant [13, 14]. On the other hand, no compelling theoretical reason for the cosmological constant to be zero has been found either. Schemes have been invented where the vacuum expectation value of a scalar field (“quintessence”) varies which time so as to track the matter energy [3]. It may be possible to distinguish between

this possibility and a true cosmological constant with future high-precision supernova and/or CMB data.

4.5. *The cosmic microwave background*

Perhaps the strongest argument in favour of non-baryonic dark matter comes from structure formation and the cosmic microwave background. As already mentioned, the high degree of isotropy and the nearly gaussian and scale-invariant nature of the anisotropy of the CMB gives credence to inflation which in turn generically predicts $\Omega_0 = 1$. In addition, it has proven to be very difficult to bridge the epoch of the emission the CMB (some 300 000 years after the big bang) and that of formation of large scale structure in the universe without the help of non-baryonic matter.

The basic picture is simple: The COBE satellite observations of the anisotropy of the microwave background at the level of a few times 10^{-5} gives the normalization of the density perturbations in the universe at that epoch, at a redshift of around $z \sim 1100$ when the universe quite suddenly became transparent due to the recombination of electrons with hydrogen and helium nuclei. According to the standard theory of structure formation in the expanding universe, the gravitational instability caused an adiabatic growth of these primordial fluctuations with time. However, when the fluctuations were small, this growth was only linear in the scale factor a , and could start only when the universe was matter-dominated. With baryons only, this occurred roughly at the time when the CMB radiation was emitted. This means that it is very difficult to understand how the highly non-linear structures observed today could exist, since they have evolved much more than the factor 1100 that linear growth could yield. This schematic picture is verified by large numerical simulations of structure formation.

Non-baryonic dark matter helps since if it exists, matter domination occurred earlier, causing also the perturbations to start to grow earlier. When the radiation pressure on the baryons was released after the CMB epoch, the baryons could fall into the gravitational wells already formed by the non-baryonic dark matter. In fact, the nice agreement between the COBE observations and the predictions from inflation of an approximately gaussian scale-invariant spectrum of primordial perturbations, may also be taken as a piece of evidence in favour of inflation which predicts the presence of such fluctuations caused by quantum effects during inflation.

Recently, there has been a flurry of balloon and ground-based CMB experiments on smaller angular scales, which probe the interesting dynamics of the acoustic peaks in the primordial cosmic fluid [27]. Although one has to await longer duration balloon flights and the MAP and Planck satellite missions for precision measurements, it seems that the recent data favour a critical universe of $\Omega_0 = 1$ over an open universe of, say, $\Omega_0 = 0.3$ [16, 28]. A fortunate fact is that the location of the first acoustic peak in the power spectrum of the CMB depends on a combination of Ω_M and Ω_Λ which is orthogonal to that probed by the deep supernova surveys. Therefore, a combination of results from the two types of measurements gives much more powerful constraints

than each one separately. (See, e.g., [16, 29], where a combined analysis favours the set $\Omega_M \sim 0.4 \pm 0.1$, $\Omega_\Lambda \sim 0.6 \pm 0.1$.)

4.6. Large scale structure

In structure formation not only Ω_{DM} is important, but also the type of particle making up the dark matter. If the particle is very light (e.g., a massive but light neutrino), it will be relativistic at the time structure starts to form and will free-stream out of galaxy-sized overdense regions, so that only very large structures can form early. The terminology [30] is such that this type of particle constitutes *hot dark matter* (HDM), and structure forms top-down by the fragmentation of large structures (“pancakes”) into smaller. This behaviour is nowadays strongly disfavoured in view of observations of the distribution of galaxies at very high redshift, but a hot dark matter component at, say, the 10 % level cannot be excluded.

Massive particles (GeV or heavier) will typically move with non-relativistic velocities when they decoupled and can therefore clump also on smaller scales. This is *cold dark matter* (CDM), one important example being supersymmetric neutral massive particle discussed later. In cold dark matter scenarios, structure typically forms in a hierarchical fashion, with small clumps merging in larger ones, forming galaxy halos and successively larger structures.

Inbetween hot and cold dark matter there may exist *warm dark matter* (WDM), which could be made up of keV scale neutral particles (e.g., the supersymmetric partner of the graviton, the gravitino, in some models of supersymmetry breaking). There the inverse of the mass scale of the particle defines a length scale of structure formation below which early structure is suppressed. Warm dark matter is not particularly in favour at the moment, both for particle physics and structure formation reasons, but the possibility should be kept in mind.

There are particles, like the axion, which behave like cold dark matter although they most likely are very light. This is due to the nonthermal way they were produced.

Although the details of the structure formation history of the universe probably will remain unclear until the next generation of microwave background measurements and digital sky surveys are available, the formerly (in the 1980’s) so popular “Standard Cold Dark Matter” (SCDM) model with $\Omega_{CDM} = 0.95$, $\Omega_B = 0.05$, the slope parameter of the scale invariant primordial power spectrum $n = 1$, and $h = 0.5$ is now disfavoured as observations have become more refined. The main problem is that normalization to the COBE spectrum at the largest scales causes by approximately a factor of 2 too much power on the smaller scales probed by galaxy and cluster surveys. However, with only small modifications such as adding an HDM component, tilting the primordial spectrum to 0.8 – 0.9, decreasing h below 0.5 or a combination thereof one can get a quite satisfactory description of the data [31].

A recent important piece of evidence in favour of the existence of cold dark matter, with an estimated $\Omega_M \sim 0.3$ (for a flat universe) or 0.5 (for an open universe) comes from

observations of the Lyman- α forest [32], combined with the observed mass function of galaxy clusters, clearly necessitating a substantial amount of non-baryonic dark matter. Combining data from cluster abundances, the CMB and the IRAS infrared galaxy catalog, a range $0.30 < \Omega_M < 0.43$ can be inferred [33].

Still on very large scales, analyses of the peculiar velocity “flow” of large clusters and other structures seem to need a lot of gravitating matter for its explanation, at least $\Omega_M > 0.4$ [25]. The peculiar velocity field obeys the equation

$$\nabla \cdot \mathbf{v} = \frac{-\Omega_M^{0.6}}{b} \left(\frac{\rho - \langle \rho \rangle}{\langle \rho \rangle} \right), \quad (28)$$

where $b = \delta\rho_{Gal}/\delta\rho_M$ is the “biasing” parameter which tells how light traces mass. The combination $\Omega_M^{0.6}/b$ is determined by the analysis of [25] to be 0.89 ± 0.12 , which is consistent with $\Omega_M = 1, b = 1$. Using the theoretical limit $b > 0.75$, a 95 % c.l. limit of $\Omega_M > 0.33$ can be given.

4.7. Galaxy clusters

The analysis of galaxy clusters is starting to converge to a universal value of Ω_M . It is true that here are some indications [34] from the temperature-luminosity relation for rich clusters that a high value ($\Omega_M \sim 1$) might be needed. On the other hand [35, 36, 37] most dynamical estimates are more consistent with a lower value, $\Omega_M \sim 0.2 - 0.3$ on cluster scales.

Of special importance is the large amount of X-ray emitting hot gas present in rich galaxy clusters. These systems are large enough that the baryon fraction should be a good tracer of $r_B = \Omega_B/\Omega_M$. Estimates [38] give a value of $r_B \sim 0.1 - 0.2$, which combined with the BBN determination of Ω_B gives $\Omega_M \sim 0.2$ if the high deuterium measurement [39] is correct, $\Omega_M \sim 0.5$ for the low deuterium abundance case [40], with probably rather large systematic uncertainties related to the limited understanding of how clusters formed and how the gas thermalized.

Also the microwave background can be used to extract Ω_M , namely through the Sunyayev-Zel’dovich (SZ) effect, by which the CMB gets spectrally distorted through Compton scattering on hot electrons in galaxy clusters. This effect of course depends on the baryonic fraction of the cluster and could therefore give an estimate of Ω_M with the same assumption that the baryon fraction of clusters is a fair sampling of the cosmological baryon fraction. With present SZ data, a value of $\Omega_M h \sim 0.25$ is obtained [41].

It is interesting that cluster mass estimates based on gravitational lensing, X-ray emission, the SZ effect and galaxy motions all give similar mass estimates within about a factor of two.

4.8. The need for non-baryonic dark matter

To summarize at this point: A variety of independent estimates of the matter density in the universe point to a value larger than the maximal value provided by baryons

alone according to nucleosynthesis. The need for nonbaryonic dark matter is therefore striking. If the “natural” theoretical prediction $\Omega_M = 1, \Omega_\Lambda = 0$ is fulfilled is a different question, for which most of the observational data today do not give support, except some weak indications at the largest scales. If one accepts, as seems implied by the deep supernova surveys, a non-vanishing cosmological constant Λ , then a satisfactory description of most cosmological observations is obtained by a “ Λ CDM model” with $\Omega_B \sim 0.05, \Omega_{\text{CDM}} \sim 0.25, \Omega_\Lambda \sim 0.7$, see Fig.2.

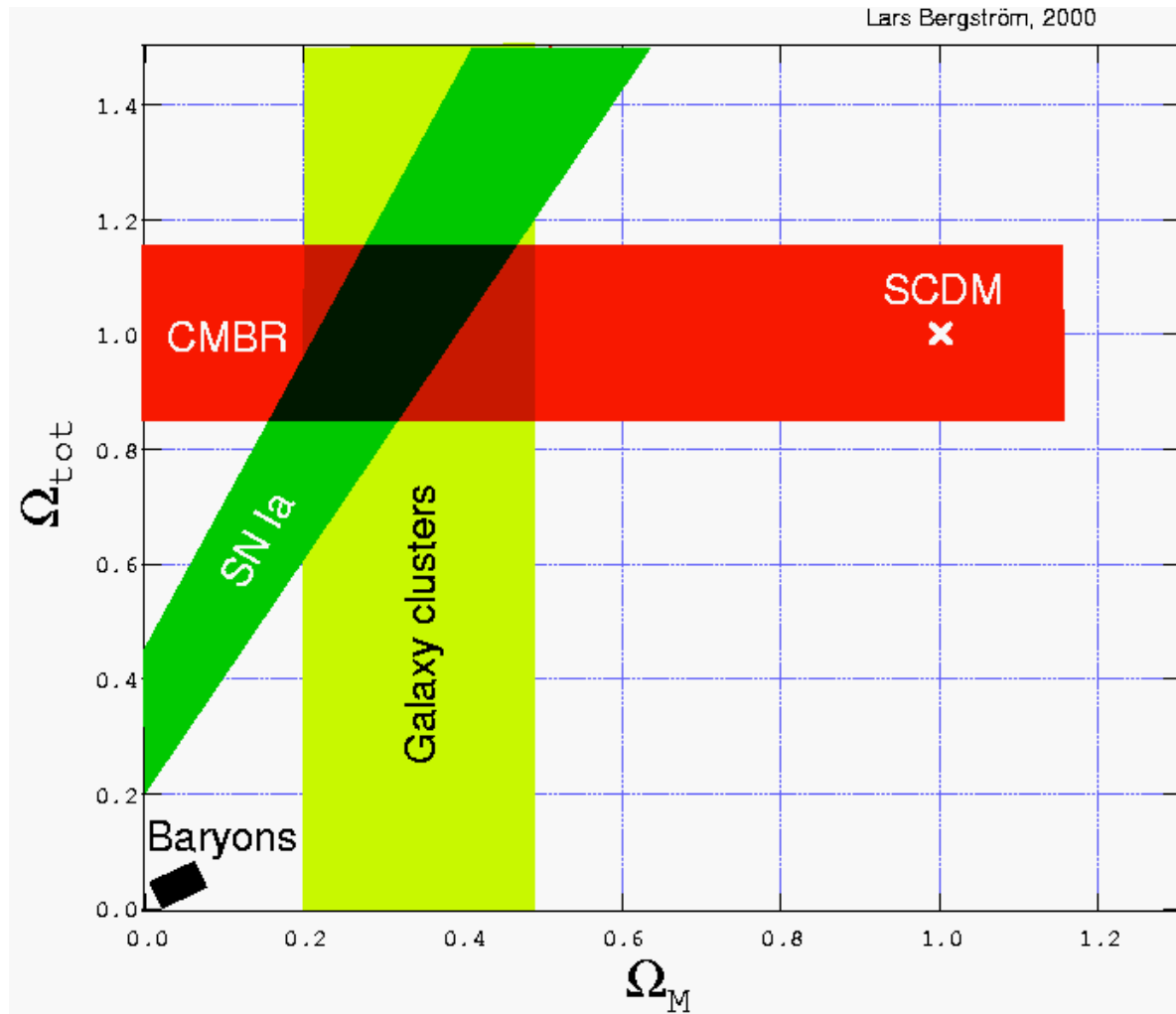


Figure 2. Approximate best-fit coincidence regions in the Ω_M – Ω_{tot} plane (assuming that only Ω_M and Ω_Λ contribute to Ω_{tot}), from the joint analysis of Type Ia supernovae [4] (diagonal shaded band), cosmic microwave background radiation [28] (horizontal band) and X-ray cluster mass measurements [38] (vertical band). As can be seen, there is a concordance region for $\Omega_M \sim 0.3, \Omega_{\text{tot}} \sim 1$ (i.e., $\Omega_\Lambda \sim 0.7$). Also shown is a region at very small Ω_M which bounds the baryons-only contribution according to big bang nucleosynthesis [1]. The formerly popular “Standard CDM” model, SCDM, is shown as the cross at $\Omega_{\text{tot}} = \Omega_M = 1$.

4.9. Problems with Cold Dark Matter

There is thus compelling evidence for dark matter on large scales in the universe, and big bang nucleosynthesis forbids the larger part of it to be baryonic. The present-day “best fit” model is a flat Λ CDM model with $h \sim 0.65$, $\Omega_M \sim 0.3$ and $\Omega_\Lambda \sim 0.7$, where baryons only contribute $\Omega_B \sim 0.05$ to Ω_M , the rest being due to cold, non-baryonic dark matter. Although this model fits most of the cosmological data remarkably well, there are some reasons for caution.

One potential problem for the Λ CDM model, as for most other versions of CDM models, is that it predicts galaxy halos that have a steeper density profile in the inner parts than may be observed [42, 43]. Also, N-body simulations seem to give much more substructure of dark matter within clusters and galactic halos than what is observed, e.g., in terms of the number of dwarf satellite galaxies to the Milky Way. It is not clear, however, how serious these problems are in view of the large uncertainties present in the N-body simulations of structure formation as regards, e.g., the shape and slope of the primordial spectrum of initial perturbations [44]. The situation concerning these numerical simulations is presently confused, with different groups reaching different conclusions concerning, e.g., the dark matter density profiles near the centres of galaxies. This is a problem we will return to when discussing experimental signatures of various cold dark matter particle candidates. It has recently been proposed [45], that the problem can be circumvented if the dark matter is self-interacting with rather large cross section but interacts weakly with ordinary matter and also has a suppressed annihilation rate. It remains to be seen however, if a realistic particle physics scenario can be found for this type of model.

A major observational difficulty is to extract the rotation curve in the inner parts of galaxies. One recent analysis [46] finds, for instance, that if one takes beam smearing into account the density profiles of low surface brightness galaxies are indeed consistent with having a steep central cusp, in contrast to previous claims. This is a field where more refined observations are clearly needed.

The introduction of the cosmological constant adds a new parameter which of course makes a fit to some sets of cosmological data easier (and it has to be reminded that most of the data may have large systematic uncertainties). From a theoretical point of view, other modifications of the parameters may then be preferable, such as, for example, lowering h to well below 0.5 [47]. This does not seem easy to do given the concurrence of several methods which give the “canonical” range of 0.65 ± 0.15 . The point made here, however, is that there is no simple cosmological model which does not have problem with at least some sets of data. In that situation it may be wise to keep several possibilities open, while awaiting data of higher precision.

5. Baryonic Dark Matter

5.1. *Big bang nucleosynthesis*

The BBN limit in Eq. (27) is important, since it implies that if observations give a value of the total energy density above the BBN value, non-baryonic dark matter has to be present (or baryons have to be hidden in some non-standard way at the time of nucleosynthesis), even if the total Ω_M turns out to be less than unity. Indeed, we have seen that there are several independent indications that $\Omega_M > 0.1$ (and hardly any estimates at all that fall below that limit). Of course, it has long been recognized that even the minimum value of Ω_B allowed by BBN is higher than the contribution from luminous baryons so that there also exists a dark matter problem for baryons - a lot of baryonic matter has to be hidden.

5.2. *The Milky Way disk*

The distinguishing feature between baryonic and non-baryonic matter is that the former, due to its coupling to the electromagnetic field, is able to emit light, i.e. radiate. As a consequence of this, energy is dissipated which is why baryonic matter in galaxies usually is concentrated to a bulge and/or bar near the center, and for spiral galaxies also in the form of a thin disk. Non-baryonic dark matter, however, most plausibly consists of electrically neutral, non-interacting particles and is therefore unable to condense by dissipation. On the other hand, dark matter structure can evolve in several ways under the influence of gravity. Besides the hierarchical clustering seen in simulations of dark matter structure formation, there will also be an interplay between the baryonic and non-baryonic components, e.g., infall and accretion of dark matter and gas onto galaxies and perhaps also on smaller substructures. It may therefore be interesting to estimate the amount of dark matter also on the smaller scales represented, e.g., by the galactic disks.

For the Milky Way, Oort [48] was the first to give estimates based on the motions of stars perpendicular to the disk. This analysis seemed to necessitate dark matter in the solar neighbourhood in the disk. After some controversy, this suggestion was however convincingly refuted by Kuijken and Gilmore [49] who devised a method which used the full three-dimensional distribution of velocities and positions of the tracer stars. They showed that the dynamical effects on the tracers can be entirely accounted for by visible material, leaving little room for disk dark matter (see [50] for an extensive review of the evidence for dark matter on various scales in galaxies).

5.3. *Hidden baryons - gas*

Apart from the relatively large amounts of hot X-ray emitting gas in clusters, the main baryonic component of the universe may be diffusively distributed gas inbetween galaxies and clusters. This is very difficult to detect at low redshifts using presently available methods. However, an analysis of the absorption of light from distant quasars due to intervening gas shows that the amount of hydrogen and helium gas corresponds well to

the nucleosynthesis prediction [51].

5.4. Hidden baryons - MACHOs

It is not excluded that a large amount of baryonic mass may be hidden in galactic halos in the form of sub-solar mass objects, MACHOs [52]. For such objects, the clever technique of microlensing has been used as a tool. The idea is to monitor 1 to 10 million stars in a satellite galaxy, e.g., the Large Magellanic Cloud (LMC) or Small Magellanic Cloud (SMC). The intensity of one of these background stars will rise in a typical, time-symmetric and achromatic fashion during a few days, weeks, or months (depending on the mass and transverse velocity of the intervening object) if an object such as a non-luminous star passes the line-of-sight to the star [53], if such stars make up a sizeable fraction of the Galactic halo. Indeed, such microlensing events were reported by two collaborations [54, 55] soon after the observational programmes started.

However, given the optical depth for microlensing observed towards the LMC [55, 56], the most likely fraction of the halo mass given by MACHOs is not larger than around 20%. In fact, it could be much smaller if debris from tidal stripping of the LMC itself or other dwarf satellites happens to lie in the line-of-sight, as indicated by some observations [57], or if LMC is more elongated along the line-of-sight than previously thought [58].

A problem with the MACHO hypothesis, even if the events are due to a halo population, is to understand what the lensing objects could be [59, 60]. As even low-mass stars ($\sim 0.1M_{\odot}$) radiate at some level, one may use the very stringent limits from photometric surveys [61] of Abell clusters to rule out a halo contribution of more than a percent of those objects. Also, if stellar remnants are cosmologically important as dark matter objects, their progenitors would have generated a diffuse infrared flux throughout the universe, which would cause absorption of TeV gamma rays. As such gamma rays have been observed from objects at redshifts above 0.03, a stellar remnant population of the required abundance seems very unlikely [62].

Since the EROS microlensing experiment [55] rules out the region of less massive stars (down to 10^{-5} solar masses), it is difficult to fit conventional star-like objects into the hypothesis of a MACHO halo, regardless of the very unusual mass function that would be needed. In fact, evidence against a non-standard mass function for stars is mounting, since recent measurements of the distribution of stellar masses in a wide variety of environments indicate a universal function, and one which supports the canonical view that low-mass objects cannot be numerous enough to be dynamically important in galaxy halos [63].

Thus, despite early optimism of at least a partial solution of the dark matter problem when the first events were reported using this elegant microlensing technique, it may seem now that these experiments are of more interest to stellar population studies, and for determining the distribution of stars in the Milky Way and in the Magellanic Clouds.

5.5. Exotic baryonic matter

Even though there is not much at present which points to a major component of dark matter being of baryonic form, one cannot entirely rule out some exotic scenarios. Since many of these invoke “conventional” matter, such as difficult to detect (and exclude) cold molecular clouds or very low mass stars with an extremely fine-tuned mass function, a major yet unsolved problem for these models is to circumvent the nucleosynthesis bound (or to adopt the unlikely hypothesis that we live in a very low density universe).

A form of baryonic dark matter which could avoid the BBN bound is primordial black holes [64]. If such objects formed before nucleosynthesis (e.g., at the quark-hadron phase transition) they would not have a noticeable effect on the light element abundances. There are, however, many problems with such a scenario. Recent thinking in particle physics puts the strongly first order transition needed at low probability. Also, the mass spectrum of primordial black holes must be peaked at those particular masses where observational constraints happen to be the weakest.

6. Distribution of dark matter

6.1. Galactic halos

On galactic scales and smaller, the classical tests of the mass distribution provided by rotation curves continue to be refined. A compilation of almost 1000 rotation curves led to the conclusion that dark matter indeed is present in large amounts [65]. The problem of how dark matter is distributed in halos of galaxies and galaxy clusters is an important one for the purpose of determining strategies for the detection of the various candidates, as we will see. Unfortunately, the available data on the structure of the Milky Way do not constrain the dark matter halo density profile very well [66].

For a spiral galaxy which has a spherically symmetric overall mass distribution, Newton’s laws of gravity give for the rotation velocity of a tracer star, or neutral hydrogen, at distance r from the centre

$$\frac{v_{\text{rot}}^2}{r} = \frac{G_N M(r)}{r^2}, \tag{29}$$

where v_{rot} is the rotation velocity and $M(r)$ is the total mass of the galaxy interior to r . This gives

$$M(r) = \frac{v_{\text{rot}}^2 r}{G_N}, \tag{30}$$

so that a constant rotation velocity, which is usually observed for spiral galaxies over a large range of r implies a halo mass which grows linearly with r . Realistically, this growth can not extend arbitrarily far. For mass distributions obtained from numerical simulations of structure formation with cold dark matter, the growth of mass eventually becomes only logarithmic until a halo starts to overlap with one of a nearby galaxy.

A phenomenological form of the dark matter halo mass density distribution with free parameters which can be chosen to reproduce most measured rotation curves is given by

$$\rho(r) \propto \frac{\rho_c}{(r/a)^\gamma [1 + (r/a)^\alpha]^{(\beta-\gamma)/\alpha}}, \quad (31)$$

where a is a dimensionful parameter related to the core radius of the halo. Among the many shapes contained in this family of density curves can be mentioned the isothermal profile with a core (model S_p in the following), $(\alpha, \beta, \gamma) = (2, 2, 0)$; the Navarro-Frenk-White (NFW) model $(\alpha, \beta, \gamma) = (1, 3, 1)$, and the mildly singular models found in [67], $(\alpha, \beta, \gamma) = (2, 3, 0.2)$ (model K_a), $(\alpha, \beta, \gamma) = (2, 3, 0.4)$ (model K_b). All of these are capable of reproducing the observed rotation curves of most galaxies over a large range of radii, but have quite different behaviour at very small or very large radii.

If the Galactic halo consists of non-baryonic dark matter particles, the local value ρ_0 of the dark matter density at our galactocentric distance R_0 is of interest to various detection experiments. Both of these quantities are presently uncertain, in particular ρ_0 which also depends on the shape of the density profile. In Fig. 3, from [68], it is shown how ρ_0 is changing as a function of the “core radius” a for some of the models contained in the family given in Eq. (31) which can describe the gross features of our Galaxy. As can be seen, the variation is large but a range of

$$\rho_0 \sim 0.2 - 0.5 \text{ GeV/cm}^3 \quad (32)$$

covers most of the possibilities. In this analysis, a spherical halo has been assumed. If a rotating and/or flattened halo is considered, the range of reasonable values of the local halo density may be somewhat larger [69, 70].

Usually one takes the local galactic velocity distribution of the dark matter particles to be a truncated gaussian, which in the Earth frame moving at speed v_O relative to the galactic halo means

$$f(v) = \frac{1}{\mathcal{N}_{\text{cut}}} \frac{v^2}{uv_O\sigma} \left\{ \exp\left[-\frac{(u-v_O)^2}{2\sigma^2}\right] - \exp\left[-\frac{\min(u+v_O, v_{\text{cut}})^2}{2\sigma^2}\right] \right\} \quad (33)$$

for $v_{\text{esc}} < v < \sqrt{v_{\text{esc}}^2 + (v_O + v_{\text{cut}})^2}$ and zero otherwise, with $u = \sqrt{v^2 + v_{\text{esc}}^2}$ and

$$\mathcal{N}_{\text{cut}} = \frac{v_{\text{cut}}}{\sigma} \exp\left(-\frac{v_{\text{cut}}^2}{2\sigma^2}\right) - \sqrt{\frac{\pi}{2}} \text{erf}\left(\frac{v_{\text{cut}}}{\sqrt{2}\sigma}\right). \quad (34)$$

Typical values are for the halo line-of-sight velocity dispersion $\sigma = 150$ km/s, the galactic escape speed $v_{\text{cut}} = 600$ km/s, the relative Earth-halo speed $v_O = 230$ km/s (a yearly average) and the Earth escape speed $v_{\text{esc}} = 11.9$ km/s. The small variation of the relative Earth-halo speed with season will cause a possible annual modulation in the detection rate in Earth-based detectors for dark matter particles [71] as discussed further in Section 9.1.

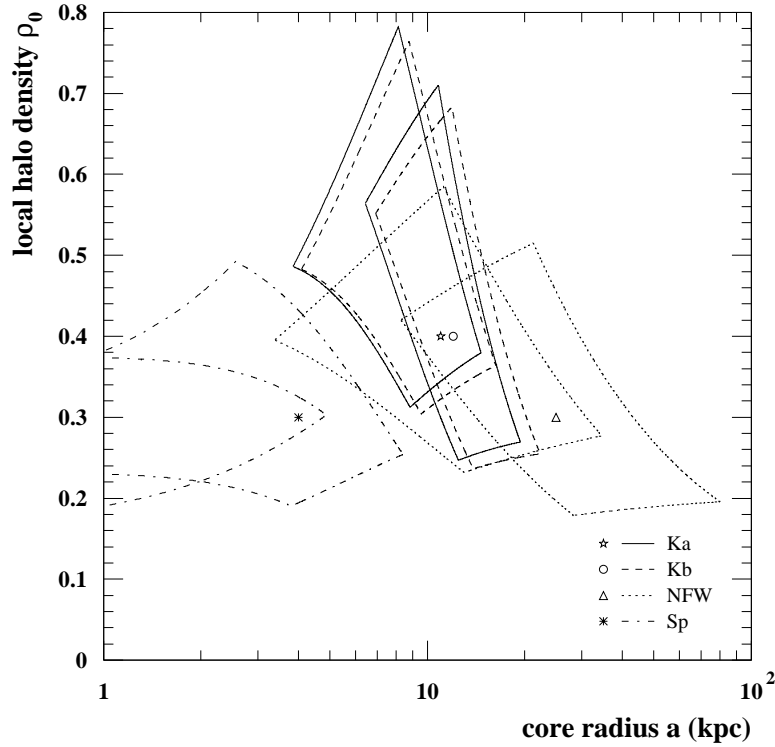


Figure 3. Allowed values of the parameters ρ_0 , the local halo density, and a , the core radius, for some commonly used halo profiles discussed in the text. The allowed regions depend on the galactocentric distance of the solar system R_0 ; plotted are regions corresponding to $R_0 = 8.5$ kpc which extend to lower values of a and to $R_0 = 7.1$ kpc which allow higher values of a . The markers indicate the halo profiles which are considered in Section 9.3.1. Figure prepared by P. Ullio, for more details, see [68].

6.2. Dwarf and low surface brightness galaxies

A very interesting class of objects is provided by low surface brightness galaxies and dwarf spiral and irregular galaxies, which seem to be completely dominated by dark matter [72]. A couple of these have unusual rotation curves which could perhaps be interpreted as being due to a combination of MACHOs and nonbaryonic dark matter [73].

Dwarf spirals are interesting, since they have rotation curves which are clearly rising well beyond the scale length of the luminous disk. In the local group, M33 at a distance of only around 0.8 Mpc gives a good opportunity to study the rotation curve since it has HI gas which can be traced out to large distances from the center. This is shown in Fig. 4, where the rotation curve measurements extracted from [74] are shown superimposed on an optical image of the galaxy. Also shown is the contribution to the

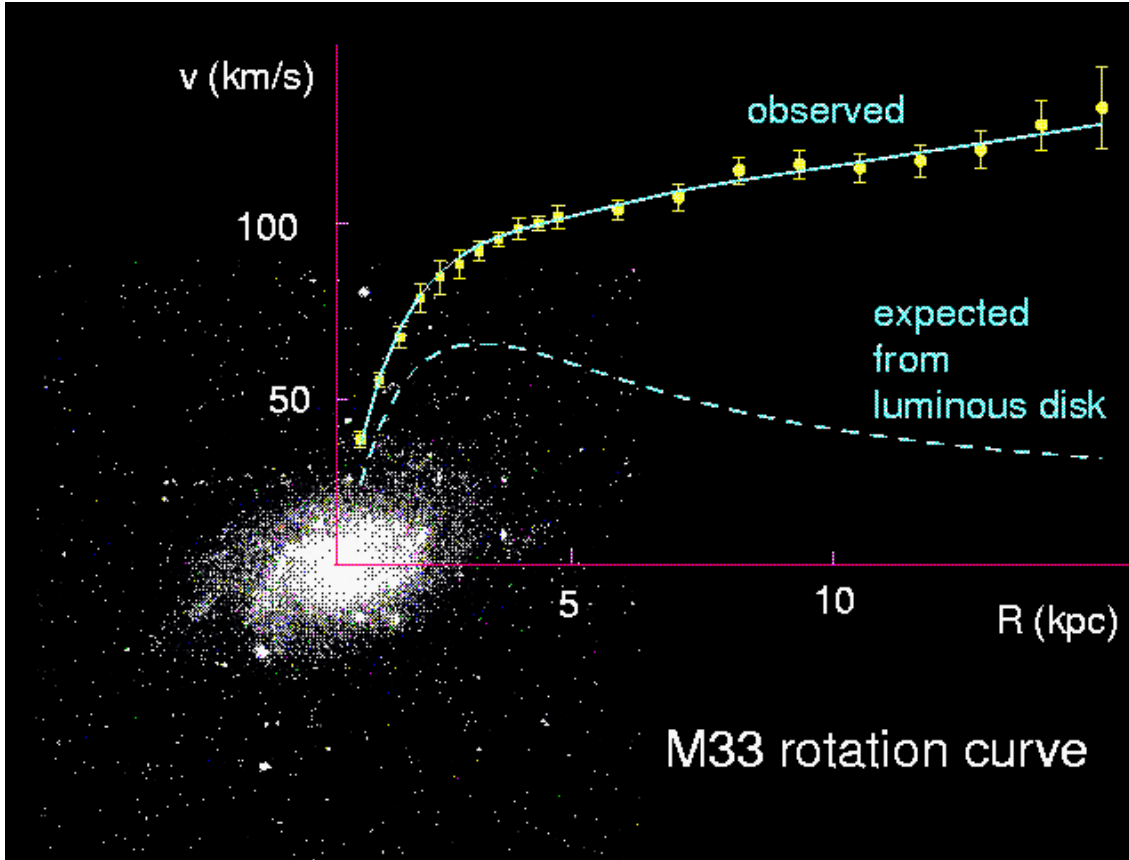


Figure 4. Observed H I rotation curve of the nearby dwarf spiral galaxy M33 (adapted from [74]), superimposed on an optical image [75]. The dashed line shows the estimated contribution to the rotation curve from the luminous stellar disk [74]. There is also a smaller contribution from gas (not shown).

rotation curve from the luminous disk computed in [74]. (There is at large radii also a small contribution from the gas mass, not shown in the Figure.) As can be seen, the rotation curve is rising well beyond the point where Newtonian dynamics based on only the luminous mass would predict a decline. Since the curve continues to rise at the last measured points, only a lower limit to the mass of the dark halo can be given, $M \gtrsim 5 \cdot 10^{10} M_{\odot}$, more than 10 times the mass in stars and gas. It is noted in [74] that an NFW profile in fact fits the rotation curve quite well but the central concentration is lower than that predicted by an $\Omega_M = 1$ universe, perhaps indicating again the need to decrease the matter density (while allowing a cosmological constant to give a flat large-scale geometry).

7. Models for non-baryonic dark matter

Given that the total mass density of the universe seems to be higher than what is allowed by big bang nucleosynthesis for baryons alone, an important task of cosmology and particle physics is to produce viable non-baryonic candidates and to indicate how

the various scenarios can be tested observationally.

7.1. Changing the law of gravity?

It has turned out to be very difficult to modify gravity on the various length scales where the dark matter problem resides, but phenomenological attempts have been made to at least explain flat galaxy rotation curves by introducing violations of Newton’s laws (and of general relativity) [76]. Until a satisfactory alternative theory to general relativity has been found it is difficult to further comment on this option. Besides the remarkable success of the “standard” theory in accounting for perihelion motion, redshifts, gravitational lensing and binary pulsar dynamics, the overall consistency of the standard cosmology it provides the basis for, also on the largest scales, is remarkable. An example is the concordance of the mass estimates of galaxy clusters based on galaxy velocity dispersions, gravitational lensing, microwave background distortions and X-ray emission from hot intracluster gas. At present, there does not seem to exist a plausible alternative theory that can match this impressive list of successes.

In principle, there are modifications to Newtonian gravity if there exists a non-zero cosmological constant, since the energy equation for a test particle of mass m at a distance R from a homogeneous sphere of mass M gets an additional term proportional to Λ ,

$$E = \frac{1}{2}m\dot{R}^2 - \frac{G_N M m}{R} - \frac{\Lambda}{6}mR^2, \quad (35)$$

(see [6]) showing the attractive nature of the extra force for $\Lambda < 0$. However, this additional term is some four orders of magnitude too small to have measurable effects in galactic systems, given the current observational estimates of Λ [77]. In addition, the observationally favoured value of Λ is positive and thus causes repulsion instead of attraction.

7.2. Particle Dark Matter

We have seen that many independent observations point to the existence of non-baryonic dark matter in the universe. Even in the absence of observations, we noticed in Sec. 3 that it may not be unexpected that massive, electrically neutral, weakly interacting and long-lived particles make up a substantial fraction of the average cosmic mass density. If such a massive particle species has roughly the same type of gauge couplings as the known quarks and leptons, it must have been produced in large abundances in the earliest universe when the thermal energies were high enough to produce it in collisions between ordinary particles.

As the universe expanded, the temperature decreased and eventually the production was cut off because of the lack of sufficient energy of the colliding particles in the primordial plasma. Also, the probability that particles of this new type would collide with each other and annihilate decreased rapidly as their number density was

diluted by the expansion. This generic mechanism was investigated first for neutrinos [78, 79, 80, 81] but is generally valid, also for heavier particles as discussed in Section 3.

There are slight modifications needed for various types of possible dark matter candidates. For example, if the particle is different from the antiparticle, it may be that there exists an asymmetry which can make the relic number density higher than if there would be a perfect symmetry. This may allow for a relic density which is higher than the estimate in Eq. (20) even if the annihilation cross section is large. In fact, such an asymmetry must have existed for the baryons, because otherwise baryons would have been almost completely annihilated by antibaryons due to the large annihilation cross section caused by the strong interaction, making a very different universe from that observed. From BBN considerations, one finds that the baryon-antibaryon asymmetry must have been of the order of one part in 10^9 . The origin of this CP violating and baryon number violating asymmetry is still unknown, and probably one needs to go beyond the standard model of particle physics to explain it.

If the particle is identical to the antiparticle, this uncertainty of the amount of asymmetry does not appear. The electrically neutral spin-1 particles γ and Z^0 are examples of such self-charge conjugate particles. It is possible also for a neutral spin-1/2 particle to be its own antiparticle, a so-called Majorana fermion. This is the generic case for supersymmetric particles to be discussed in Section 8.

For Majorana and other self-conjugate particles, and for particles where the asymmetry is zero, the calculation of the relic density proceeds as in Section 3, and the relic density can usually be estimated from Eq. (20).

Assuming a thermal production process in the early universe, there is an upper limit to the mass of a stable relic particle [82]. This comes about because unitarity precludes the annihilation cross section of particles of mass M , spin J and relative velocity (in the centre of mass frame) v_{rel} from being larger than $4\pi(2J + 1)/(M^2 v_{\text{rel}}^2)$. Using the estimated v_{rel} at freeze-out, it is found that M cannot exceed around 340 TeV. The most favoured heavy dark matter candidate, the lightest supersymmetric particle, always has a mass much below this limit in the minimal models. There may be a possibility to evade the unitarity bound and accept even extremely heavy particles as dark matter candidates if, for instance, they are not absolutely stable (so that the formula in Eq. (20) does not apply), or if the production mechanism is non-thermal [83, 84].

7.3. Particles with only gravitational interactions

Although there are particle physics motivated dark matter candidates which have non-negligible couplings to ordinary matter, and which therefore are in principle detectable through other interactions than gravity, there is always the possibility that the dark matter interacts only gravitationally, or extremely weakly, with ordinary matter. In fact, this possibility may arise in different string theory-inspired scenarios [85, 86]. The possibility to confirm or experimentally rule out such presently very speculative models is uncertain to say the least, and we will not discuss them further.

7.4. Massive neutrinos

Of the many candidates for non-baryonic dark matter proposed, neutrinos are often said to have the undisputed virtue of being known to exist. Actually, this is a statement which needs some qualification because neutrinos can only be dark matter candidates if they are massive. For this to be true, both left-handed and right-handed neutrino states are needed, and the latter are not known to exist (in the minimal Standard Model of particle physics the right-handed neutrino is simply absent). In principle, one can construct a mass term from only the left chirality neutrino field, but this gives a Majorana type mass which violates lepton number by two units, and in the Standard Model $B - L$ is exactly conserved. Also, one would have to introduce an isotriplet Higgs field in addition to the isodoublet present in the Standard Model.

Non-zero neutrino masses, if established, would thus be an indication of physics beyond the Standard Model. Since there exists a number of indications that the Standard Model cannot be the final theory, it would not be a big surprise if neutrinos are massive. As the direct experimental limits on neutrino mass show [87],

$$\begin{aligned}
 m_{\nu_e} &< 15 \text{ eV} \\
 m_{\nu_\mu} &< 0.19 \text{ MeV} \\
 m_{\nu_\tau} &< 18.2 \text{ MeV}
 \end{aligned}
 \tag{36}$$

the neutrino masses have to be much smaller than the corresponding quark and charged-lepton masses. An intriguing explanation of this fact could be given by the so-called see-saw mechanism, where a right-handed Majorana mass M , at a large scale $\propto M_{GUT} \sim 10^{15\pm 2}$ GeV modifies through mixing the usual Dirac-type mass m_D of the lightest state to $m_D^2/M \ll m_D$. In the simplest versions of this scheme, the neutrino masses would scale as the square of the corresponding charged-lepton masses. There are variants (e.g., in models of loop-induced neutrino masses) where neutrino masses are instead linearly related to the charged-lepton masses.

Indeed, there exist several indications that neutrinos are not massless. Although the direct kinematical measurements of neutrino masses have given values consistent with zero, evidence from neutrino oscillation experiments is mounting that neutrinos oscillate in flavour and hence must possess non-zero masses. To give a cosmologically interesting contribution to Ω , a relatively narrow range $m_\nu \sim 1 - 50$ eV is required (see Eq. (19)). A neutrino heavier than that would overclose the universe unless $m_\nu > 3$ GeV, when it would be non-relativistic at freeze-out with a small enough relic abundance to act as Cold Dark Matter. This is ruled out for Dirac neutrinos by accelerator and direct detection data up to the TeV range. At the other mass end, a neutrino lighter than 1 eV would only give a small and dynamically not very important contribution to Ω .

Of the various experimental indications of neutrino oscillations, only the LSND results [88] seem to be in the cosmologically interesting range, with $\Delta m^2 \sim 1 - 6 \text{ eV}^2$. These results, however, need independent confirmation from other experiments. In fact, large portions of the region of mass differences and mixing angles indicated by LSND have been excluded by the KARMEN experiment [89]. A definitive answer will probably have to await new experiments such as BooNE at Fermilab [90].

The solar neutrino problem, which in view of new helioseismological data does not seem to be solvable by changing the standard astrophysical solar model [91], and thus presents rather compelling evidence for oscillations, indicates solutions with very small Δm^2 . This would imply small absolute values of neutrino masses unless there exists a mass degeneracy of unknown origin between neutrinos. Such a degeneracy is, however, easily destroyed by higher order quantum corrections, and therefore seems contrived [92].

Likewise, the atmospheric neutrino anomaly, recently confirmed by Super-Kamiokande data, has a preferred solution with a Δm^2 of only a few times 10^{-3} eV^2 . Seen already in the smaller Kamiokande detector [93], as well as in IMB [94] and recently also confirmed by Soudan-2 [95] and MACRO [96], what is observed is a deficit in the “ratio of ratios”, $r \equiv (\nu_\mu/\nu_e)_{data}/(\nu_\mu/\nu_e)_{MC} \sim 0.6$. The interpretation in terms of neutrino oscillations is particularly compelling with the Super-Kamiokande data where a zenith-angle dependence of the ratio is indicated [7] with higher significance than in the other experiments. Thus it is very likely that neutrinos are indeed massive, but the mass is too small to be very significant for cosmology (although, as noted in the Introduction, neutrinos most probably contribute as much to the energy density in the universe as the visible stars). However, even if the largest neutrino mass is of the order of only a few tenths of an eV, as indicated by the atmospheric neutrino anomaly, the effects on structure formation could still be large enough to be detected in the far future by combining data from large galaxy surveys similar to the Sloan Digital Sky Survey, with precision measurements of the cosmic microwave background from the future Planck satellite [97].

There is a fundamental objection to having massive but light neutrinos as the dominant constituent of dark matter on all scales where it is observationally needed. This has to do with the fact that neutrinos are spin-1/2 particles obeying the Pauli exclusion principle. To make up the dark matter in dwarf galaxies (which are observed to be completely dominated by the dark matter component, see Fig. 4), neutrinos would have to be stacked together so tightly in phase-space that it is impossible to evade the Pauli principle. Quantitatively, Tremaine and Gunn found [98] that to explain the dark matter of a dwarf galaxy of velocity dispersion σ (usually of order 100 km/s) and core radius r_c (typically 1 kpc), the neutrino mass has to fulfil

$$m_\nu \geq 120 \text{ eV} \left(\frac{100 \text{ km/s}}{\sigma} \right)^{\frac{1}{4}} \left(\frac{1 \text{ kpc}}{r_c} \right). \quad (37)$$

This high value is, however, not consistent with the requirement $\Omega_\nu h^2 \leq 1$, which

according to Eq. (19) requires $\sum_i m_{\nu_i} < 93$ eV. The more desirable values $\Omega_\nu \sim 0.25$, $h \sim 0.65$ give in fact $m_\nu \sim 10$ eV, which violates Eq. (37) by an even larger amount. One way out of this particular problem would be if a 10 eV scale neutrino exists and is unstable on the cosmological time scale. This, however, requires exotic decay modes, since weak interaction mediated decays occur on a much longer timescale. The problem with all models for the dark matter which rely on decaying relic particles is that a considerable amount of fine tuning of the product of relic density and decay time is needed to obtain sensible values of Ω_M .

We mentioned that the upper bound in Eq. (19) on the neutrino mass is only applicable for “standard”, very light neutrinos. As a consequence of the behaviour of the freeze-out abundance and cross section as a function of mass, there is another mass range around 3 GeV where the relic density would be close to critical. Today this window is ruled out by the precision measurements at the LEP accelerator at CERN where the number of neutrino species which couple in the usual way to the Z boson has been determined to be three. The pre-LEP papers which worked out the dark matter phenomenology of such massive neutrinos (e.g., [78, 79, 80, 81]) were important, however, since they showed that a weakly interacting, massive particle (“WIMP”) could serve as cold dark matter with the required relic density.

To conclude this section about neutrinos, it seems that it is very plausible that they make up some of the dark matter in the universe (given the experimental results on neutrino oscillations), but most of the dark matter is of some other form. Particle physics offers several promising candidates for this.

7.5. Axions

In particle physics, the combined action of charge conjugation (C) and parity (P) is not an exact symmetry. For instance, higher-order weak interactions involving quarks from all three generations are believed to cause the experimentally observed small CP violation in the neutral K meson system. With the advent of quantum chromo dynamics (QCD) as the fundamental gauge theory for the strong interaction, it was found that non-perturbative effects should induce a much larger CP violation in the strong sector. However, the absence, e.g., of an electric dipole moment of the neutron puts severe upper limits on such a strong CP-violating parameter. The idea of Peccei and Quinn was to make the CP violating phase dynamical [99] by introducing a global symmetry, $U(1)_{PQ}$, which is spontaneously broken. The Goldstone boson of this broken global symmetry is the axion, which however gets a non-zero mass from the QCD anomaly, which can be interpreted as a mixing of the axion field with the π and η mesons [100, 101].

The earliest attempts, using only the standard model particles but with an enlarged Higgs sector, were soon ruled out experimentally and the “invisible axion” was invented [102, 103] with a very high mass scale of symmetry breaking and with very massive fermions carrying PQ charge. This means that only a feeble strong or electromagnetic interaction leaks out to the visible sector through triangle loop diagrams.

The phenomenology of the axion is determined, up to numerical factors, by one number only - the scale f_a of symmetry breaking. In particular, the mass is given by

$$m_a = 0.62 \text{ eV} \left(\frac{10^7 \text{ GeV}}{f_a} \right), \quad (38)$$

and the experimentally important coupling to two photons is due to the effective Lagrangian term

$$\mathcal{L}_{a\gamma\gamma} = \left(\frac{\alpha_{\text{em}}}{2\pi f_a} \right) \kappa \mathbf{E} \cdot \mathbf{B} a, \quad (39)$$

where \mathbf{E} is the electric field, \mathbf{B} is the magnetic field and κ is a model-dependent parameter of order unity.

The axion, constrained by laboratory searches, stellar cooling and the dynamics of supernova 1987A to be very light, $m_a < 0.01 \text{ eV}$ [104], couples so weakly to other matter [105] that it never was in thermal equilibrium in the early universe and it would behave today as Cold Dark Matter. The window where axions are viable DM candidates is progressively getting smaller, but still there is an acceptable range between around 10^{-5} and 10^{-2} eV where they pass all observational constraints and would not overclose the universe, see Fig. 5 taken from [106]. There is a considerable uncertainty in the relation between mass and relic density, depending on the several possible sources of axion production such as vacuum misalignment, emission from cosmic strings etc.

The coupling in Eq. (39) implies that resonant conversion between a galactic axion and an electric photon mode may take place in the presence of a strong magnetic field - not even the “invisible axion” may be undetectable [107], since the number density of these light particles in the Galaxy has to be enormous if axions are to make up the dark matter.

Fortunately, there are now two experiments [108, 109] which have the experimental sensitivity of probing much of the interesting window within the next few years.

Axions share with massive neutrinos and the supersymmetric candidates to be discussed next the attractive feature of having other, particle-physics motivated, reasons to exist besides giving a possible explanation of dark matter. Of course there are other proposed candidates which, although not yet generally accepted, could finally turn out to give the correct explanation.

8. Weakly interacting massive particles - supersymmetric particles

One of the prime candidates for the non-baryonic component is provided by the lightest supersymmetric particle, plausibly the lightest neutralino χ , to be described further in Section 8.1.

Supersymmetry seems to be a necessary ingredient in superstring theory (which is now commonly seen as one aspect of a grander theory, M-theory) which unites all the fundamental forces of nature, including gravity. In most versions of the low-energy theory there is a conserved multiplicative quantum number, R-parity:

$$R = (-1)^{3(B-L)+2S}, \quad (40)$$

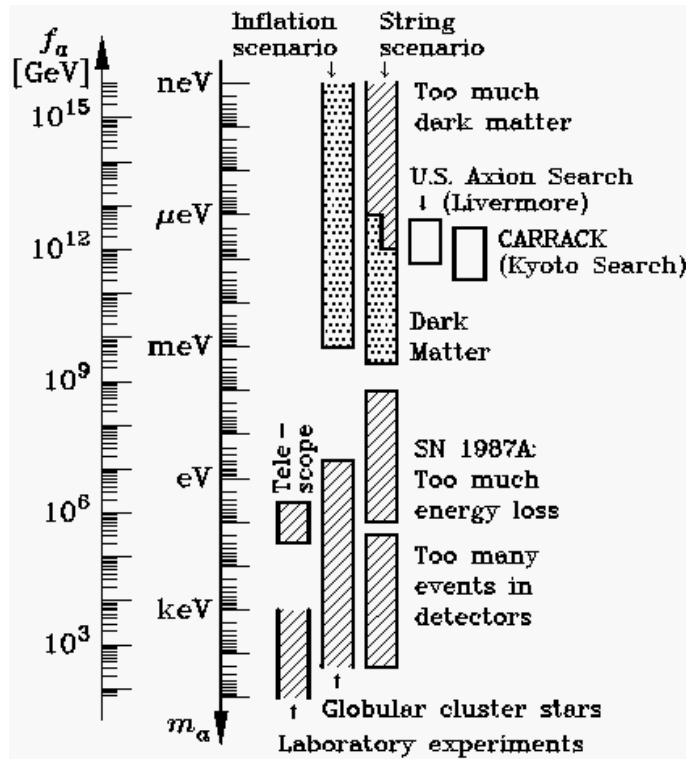


Figure 5. Astrophysical and cosmological exclusion regions (hatched) for the axion mass m_a or equivalently, the Peccei-Quinn scale f_a . An “open end” of an exclusion bar means that it represents a rough estimate. The dotted “inclusion regions” indicate where axions could plausibly be the cosmic dark matter. Most of the allowed range in the inflation scenario requires fine-tuned initial conditions. In the string scenario the plausible dark-matter range is controversial as indicated by the step in the low-mass end of the “inclusion bar.” Figure kindly provided by G. Raffelt; for more details see [104] and [106].

where B is the baryon number, L the lepton number and S the spin of the particle. This implies that $R = +1$ for ordinary particles and $R = -1$ for supersymmetric particles. This means that supersymmetric particles can only be created or annihilated in pairs in reactions of ordinary particles. It also means that a single supersymmetric particle can only decay into final states containing an odd number of supersymmetric particles. In particular, this makes the lightest supersymmetric particle stable, since there is no kinematically allowed state with negative R-parity which it can decay to.

Thus, pair-produced neutralinos in the early universe which left thermal equilibrium as the universe kept expanding should have a non-zero relic abundance today. If the scale of supersymmetry breaking is related to that of electroweak breaking, Eq. (20) shows that Ω_χ will be of the right order of magnitude to explain the non-baryonic dark matter. It would indeed appear as an economic solution if two of the most outstanding problems in fundamental science, that of dark matter and that of the unification of the basic forces, would have a common element of solution - supersymmetry.

The idea that supersymmetric particles could be good dark matter candidates

became attractive when it was realised that breaking of supersymmetry could be related to the electroweak scale, and that, e.g., the supersymmetric partner of the photon (the photino) would couple to fermions with electroweak strength [110]. Then most of the phenomenology would be similar to the (failed) attempts to have multi-GeV neutrinos as dark matter. After some early work along these lines [111, 112, 113, 114, 115], the first more complete discussion of the various possible supersymmetric candidates was provided in [116], where in particular the lightest neutralino was identified as perhaps the most promising one.

Supersymmetric dark matter should be seen at one particular realization of a generic WIMP (weakly interacting massive particle). Here weakly interacting, electrically neutral massive (GeV to TeV range) particles are assumed to carry a conserved quantum number (R -parity in the case of supersymmetry) which suppresses or forbids the decay into lighter particles. Such particles should have been copiously produced in the early universe through their weak interactions with other forms of matter and radiation. As the universe expanded and cooled, the number density of the WIMPs successively became too low for the annihilation processes to keep up with the Hubble expansion rate. A relic population of WIMPs should thus exist, and it is very suggestive that the canonical weak interaction strength is, according to detailed calculations, just right to make the relic density fall in the required range to contribute substantially to Ω .

In addition, we saw in Section 3 that WIMPs are generically found to decouple at a temperature of roughly $m_{\text{WIMP}}/20$, which means that they are non-relativistic already at decoupling and certainly behave as CDM by the time of matter dominance and structure formation, which seems to be preferred observationally.

8.1. *Supersymmetric particles*

Let us now focus on the lightest supersymmetric particle, which if R -parity is conserved, should be stable. In some early work, a decaying photino [111] or a gravitino [112] were considered, but for various reasons [116] the most natural supersymmetric dark matter candidate is the lightest neutralino χ . Thus it is a mixture of the supersymmetric partners of the photon, the Z and the two neutral CP -even Higgs bosons present in the minimal extension of the supersymmetric standard model (see, e.g., [117]). The attractiveness of this candidate, besides its particle physics virtues, stems from the fact that it is electrically neutral and thus neither absorbs nor emits light, and stable so that it can have survived since the big bang. Furthermore, it has gauge couplings and a mass which for a large range of parameters in the supersymmetric sector imply a relic density in the required range to explain the observed $\Omega_M \sim 0.3$. As we will see, its couplings to ordinary matter also means that its existence as dark matter in our galaxy's halo may be experimentally tested.

These are the good properties of neutralinos as dark matter candidates. Less attractive is the fact that virtually nothing is known about how supersymmetry is broken, and therefore any given supersymmetric model contains a large number of

unknown parameters (of the order of 100). Such a large parameter space is virtually impossible to explore by present-day numerical methods, and therefore simplifying assumptions are needed. Fortunately, most of the unknown parameters such as CP violating phases influence the properties relevant for cosmology, and for detection, very little. (In some specific cases, the effects of CP violation may be non-negligible [118].)

Usually, when scanning the large space of a priori unknown parameters in supersymmetry, one thus makes reasonable simplifying assumptions and accepts solutions as cosmologically appropriate if they give a neutralino relic density in the range

$$0.025 \lesssim \Omega_\chi h^2 \lesssim 1. \tag{41}$$

The lower limit comes from the desire to at least explain the dark matter halos of galaxies, and the upper limit is a (probably too conservative) upper limit of the observed matter density.

It should be noted, however, that the dark matter may have several components, and that supersymmetric dark matter could exist even if the lower bound in Eq. (41) is violated. Since there is in general a crossing symmetry relating a large annihilation cross section (and therefore small Ω_χ) to large scattering rates in detectors (and annihilation rates in the Galactic halo), such models giving a small relic density may in fact be interesting from the experimental point of view. Unfortunately there is, however, no simple prescription of how to go from the value of the relic density to the mass density in our Galactic halo (since that depends on the unknown formation history of the Galaxy). A phenomenological recipe has been [119] to rescale Eq. (32) by a factor $\Omega_\chi h^2 / 0.025$ if the computed relic density is smaller than the lower bound in Eq. (41). This linear rescaling of the local dark neutralino density implies for a given neutralino mass a corresponding linear decrease of scattering rates in detectors (and a quadratic decrease of annihilation rates in the halo, since the probability for two dark matter particles to annihilate is proportional to the square of the number density). It can be argued that the range in (41) is too generous. To narrow down the number of suitable supersymmetric models we will in the examples below sometimes use the more easily motivated range $0.1 < \Omega_\chi h^2 < 0.2$ (see Section 4). for the supersymmetric models to be considered and not invoke rescaling.

Besides its interesting implications for cosmology, the motivation from particle physics for supersymmetric particles at the electroweak mass scale has become stronger due to the apparent need for 100 GeV - 10 TeV scale supersymmetry to achieve unification of the gauge couplings in view of LEP results [120]. (For an extensive review of the literature on supersymmetric dark matter up to mid-1995, see Ref. [10].)

Thanks to exciting developments in string theory [121], supersymmetry has become an even more attractive feature to be expected at the doorstep beyond the Standard Model. At a more phenomenological level, supersymmetry gives an attractive solution to the so-called hierarchy problem, which is to understand why the electroweak scale at a few hundred GeV is so much smaller than the Planck scale $\sim 10^{19}$ GeV despite the

fact that there is nothing in non-supersymmetric theories to cancel the severe quadratic divergences of loop-induced mass terms. In supersymmetric theories, the partners of differing spin would exactly cancel those divergencies (if supersymmetry were unbroken). Of course, supersymmetric models are not guaranteed to contain good dark matter candidates. In particular, R -parity may not be a conserved symmetry [122] in which case there may not exist a long-lived enough particle to make up the dark matter. In the simplest models, however, and in particular in the minimal supersymmetric extension of the ordinary Standard Model that we now discuss, R -parity is conserved and the neutralino is a good dark matter candidate.

8.1.1. MSSM: The minimal supersymmetric extension of the standard model The minimal supersymmetric extension of the standard model is defined by the particle content and gauge couplings required by supersymmetry and a gauge-invariant so-called superpotential. Thus, to each particle degree of freedom in the non-supersymmetric Standard Model, there appears a supersymmetric partner with the same charge, colour etc, but with the spin differing by half a unit. The only addition to this doubling of the particle spectrum of the Standard Model concerns the Higgs sector. It turns out that the single scalar Higgs doublet is not enough to give masses to both the u - and d -like quarks and their superpartners (since supersymmetry forbids using both a complex Higgs field and its complex conjugate at the same time, which one does in the non-supersymmetric Standard Model). Thus, two complex Higgs doublets have to be introduced. After the usual Higgs mechanism, three of these states disappear as the longitudinal components of the weak gauge bosons leaving five physical states: two neutral scalar Higgs particles H_1 and H_2 (where by convention H_2 is the lighter state), one neutral pseudoscalar state A , and two charged scalars H^\pm . The Z boson mass gets a contribution from the vacuum expectation values (VEVs) of both of the doublets, but the way this division is done between the VEV v_1 of H_1 and v_2 of H_2 is not fixed a priori.

Electroweak symmetry breaking is thus caused by the neutral components of both H_1 and H_2 acquiring vacuum expectation values,

$$\langle H_1^1 \rangle = v_1, \quad \langle H_2^2 \rangle = v_2, \quad (42)$$

with $g^2(v_1^2 + v_2^2) = 2m_W^2$, with the further assumption that vacuum expectation values of all other scalar fields (in particular, squark and sleptons) vanish. This avoids color and/or charge breaking vacua. The ratio of VEVs

$$\tan \beta \equiv \frac{v_2}{v_1} \quad (43)$$

always enters as a free parameter in the MSSM, although it seems unlikely to be outside the range between 1.1 and 45 [10].

After supersymmetrization, the theory also has to contain the supersymmetric partners of the spin-0 Higgs doublets. In particular, two Majorana fermion states, higgsinos, appear as the supersymmetric partners of the electrically neutral parts of the H_1 and H_2 doublets. These can mix quantum mechanically with each other and

with two other neutral Majorana states, the supersymmetric partners of the photon (the photino) and the Z (the zino). When diagonalizing the mass matrix of these four neutral Majorana spinor fields (neutralinos), the lightest physical state becomes an excellent candidate for Cold Dark Matter.

The non-minimal character of the Higgs sector may well be the first experimental hint at accelerators of supersymmetry. At tree level, the H_2^0 mass is smaller than m_Z , but radiative (loop) corrections are important and shift this bound by a considerable amount. However, even after allowing for such radiative corrections it can hardly be larger than around 130 GeV. The successful operation of the CERN accelerator LEP at centre of mass energies above 200 GeV without observing any supersymmetric particles puts important constraints on the parameters of the MSSM. Besides the limits on the Higgs masses (presently above 100 GeV for the Standard Model Higgs), constraints on the chargino mass are significant for many dark matter searches. It has proven to be very difficult, however, to put very tight lower limits on the mass of the lightest neutralino, because of the multitude of couplings and decay modes of the next-to-lightest supersymmetric particle. The lightest neutralino can in general only be detected indirectly in accelerator experiments through the missing energy and momentum it would carry away from the interaction region. As an example of current limits, or low values of $\tan\beta$, the present lower limit on the mass of the lightest neutralino from the ALEPH collaboration is around 37 GeV [123].

The upper limit of dark matter neutralino masses in the MSSM consistent with Eq. (41) is of the order of 7 TeV [124]. Above that mass, which is still far from the unitarity bound of 340 TeV, the relic density becomes larger than the upper limit in Eq. (41). To get values for the lightest neutralino mass larger than a few hundred GeV, however, some degree of “finetuning” is necessary [125]. By making additional well-motivated but not mandatory restrictions on the parameter space, such as in supergravity-inspired models, one gets in general masses below 600 GeV [126] for the lightest neutralino.

8.1.2. Supersymmetry Breaking Supersymmetry is a mathematically beautiful theory, and would give rise to a very predictive scenario, if it were not broken in an unknown way which unfortunately introduces a large number of unknown parameters.

Breaking of supersymmetry has of course to be present since no supersymmetric particle has as yet been detected, and unbroken supersymmetry requires particles and sparticles to have the same mass. This breaking can be achieved in the MSSM by a soft supersymmetry-breaking potential which does not re-introduce large radiative mass-shifts (and which strongly indicates that the lightest supersymmetric particles should not be too much heavier than the 250 GeV electroweak breaking scale). The origin of this effective low-energy potential need not be specified, but it is natural to believe that it is induced through explicit breaking in a hidden sector of the theory at a high mass scale. The supersymmetry breaking terms are then transmitted to the visible sector through gravitational interactions.

Another possibility is that supersymmetry breaking is achieved through gauge interactions at relatively low energy in the hidden sector [127]. This is then transferred to the visible sector through some messenger fields which transform non-trivially under the Standard Model gauge group. Although this scenario has some nice features, it does not seem to give as natural a candidate for the dark matter as the “canonical” scenario, which is the one we shall assume in most of the following. See, however, Ref. [128] for some possibilities of dark matter candidates in gauge-mediated models.

Since one of the virtues of supersymmetry is that it resurrects the hope for grand unification of the gauge interactions at a common mass scale, a simplifying assumption based on this unification is often used for the gaugino mass parameters,

$$\begin{aligned} M_1 &= \frac{5}{3} \tan^2 \theta_w M_2 \simeq 0.5 M_2, \\ M_2 &= \frac{\alpha_{\text{em}}}{\sin^2 \theta_w \alpha_s} M_3 \simeq 0.3 M_3, \end{aligned} \quad (44)$$

where θ_W is the weak mixing angle, $\sin^2 \theta_W \approx 0.22$.

As mentioned, the one-loop effective potential for the Higgs fields has to be used to obtain realistic Higgs mass estimates. The minimization conditions of the potential allow one to trade two of the Higgs potential parameters for the Z boson mass $m_Z^2 = \frac{1}{2}(g^2 + g'^2)(v_1^2 + v_2^2)$ (where $g = e/\sin \theta_W$, $g' = e/\cos \theta_W$) and the ratio of VEVs, $\tan \beta$. The third parameter can further be reexpressed in terms of the mass of one of the physical Higgs bosons, for example m_A .

The neutralinos $\tilde{\chi}_i^0$ are linear combination of the neutral gauge bosons \tilde{B} , \tilde{W}_3 (or equivalently $\tilde{\gamma}$, \tilde{Z}) and of the neutral higgsinos \tilde{H}_1^0 , \tilde{H}_2^0 . In this basis, their mass matrix

$$\mathcal{M} = \begin{pmatrix} M_1 & 0 & -\frac{g'v_1}{\sqrt{2}} & +\frac{g'v_2}{\sqrt{2}} \\ 0 & M_2 & +\frac{gv_1}{\sqrt{2}} & -\frac{gv_2}{\sqrt{2}} \\ -\frac{g'v_1}{\sqrt{2}} & +\frac{gv_1}{\sqrt{2}} & 0 & -\mu \\ +\frac{g'v_2}{\sqrt{2}} & -\frac{gv_2}{\sqrt{2}} & -\mu & 0 \end{pmatrix} \quad (45)$$

can be diagonalized to give four neutral Majorana states,

$$\tilde{\chi}_i^0 = a_{i1}\tilde{B} + a_{i2}\tilde{W}_3 + a_{i3}\tilde{H}_1^0 + a_{i4}\tilde{H}_2^0 \quad (46)$$

($i = 1, 2, 3, 4$) the lightest of which, χ_1^0 or simply χ , is then the candidate for the particle making up (at least some of) the dark matter in the universe.

The coefficients in Eq. (46) are normalized such that for the neutralino

$$\sum_{j=1}^4 |a_{1j}|^2 = 1. \quad (47)$$

The properties of the neutralino are quite different depending on whether it consists mainly of gaugino ($j = 1, 2$) or higgsino ($j = 3, 4$) components. It is therefore customary to define a parameter, Z_g , which tells the size of the gaugino fraction:

$$Z_g = \sum_{j=1}^2 |a_{1j}|^2. \quad (48)$$

A neutralino is said to be gaugino-like if $Z_g \gtrsim 0.99$, higgsino-like if $Z_g \lesssim 0.01$, and mixed otherwise.

For simplicity, one often makes a diagonal ansatz for the soft supersymmetry-breaking parameters in the sfermion sector. This allows the squark mass matrices to be diagonalized analytically. Such an ansatz implies the absence of tree-level flavor changing neutral currents (FCNC) in all sectors of the model. In models inspired by low-energy supergravity with a universal scalar mass at the grand-unification (or Planck) scale the running of the scalar masses down to the electroweak scale generates off-diagonal terms and tree-level FCNC's in the squark sector. (For a discussion of this class of models, and of effects related to relaxing the assumption of universal scalar masses, see [129].) In most of the estimates of detection rates given below, we will adhere to a purely phenomenological approach, where the simplest unification and scalar sector constraints are assumed, and no CP violating phases outside those of the Standard Model, but no supergravity relations are used. This reduces the number of free parameters to be scanned over in numerical calculations to 7: $\tan\beta$, M_1 , μ , m_A , and three parameters related to the sfermion sector (the exact values of the latter are usually not very important in most of our applications). In fact, one can reduce the number of parameters further by choosing, e.g., explicit supergravity models, but this only corresponds to a restriction to a subspace of our larger scan of parameter space.

When using the minimal supersymmetric standard model in calculations of relic dark matter density, one should make sure that all accelerator constraints on supersymmetric particles and couplings are imposed. In addition to the significant restrictions on parameters given by LEP (e.g., [130, 123]), the measurement of the $b \rightarrow s\gamma$ process is providing important bounds [131, 132, 133], since supersymmetric virtual particles may contribute significantly to this loop-induced decay. These bounds are also included in the following analysis.

The relic density calculation in the MSSM for a given set of parameters is nowadays accurate to a few percent or so. A recent important improvement is the inclusion of coannihilations, which can change the relic abundance by a large factor in some instances [124, 126].

In Fig. 6 we show the calculated values of $\Omega_\chi h^2$ versus mass for a large sampling of the 7-dimensional supersymmetric parameter space (described more in detail in [134] and references therein). As can be seen, there is a very large range of $\Omega_\chi h^2$ possible, but the interesting range between, say, 0.1 and 0.2 (assuming $h \sim 0.7$) is comfortably reached by a large set of models, as anticipated in the discussion after Eq. (20). It is important to notice that the structures that can be seen in the Figure are caused mainly by the way the supersymmetric parameter space has been sampled. For instance, the almost straight diagonal band on the lower side is made up of models which are nearly pure higgsinos. By making a cut on the maximal higgsino fraction this band would disappear.

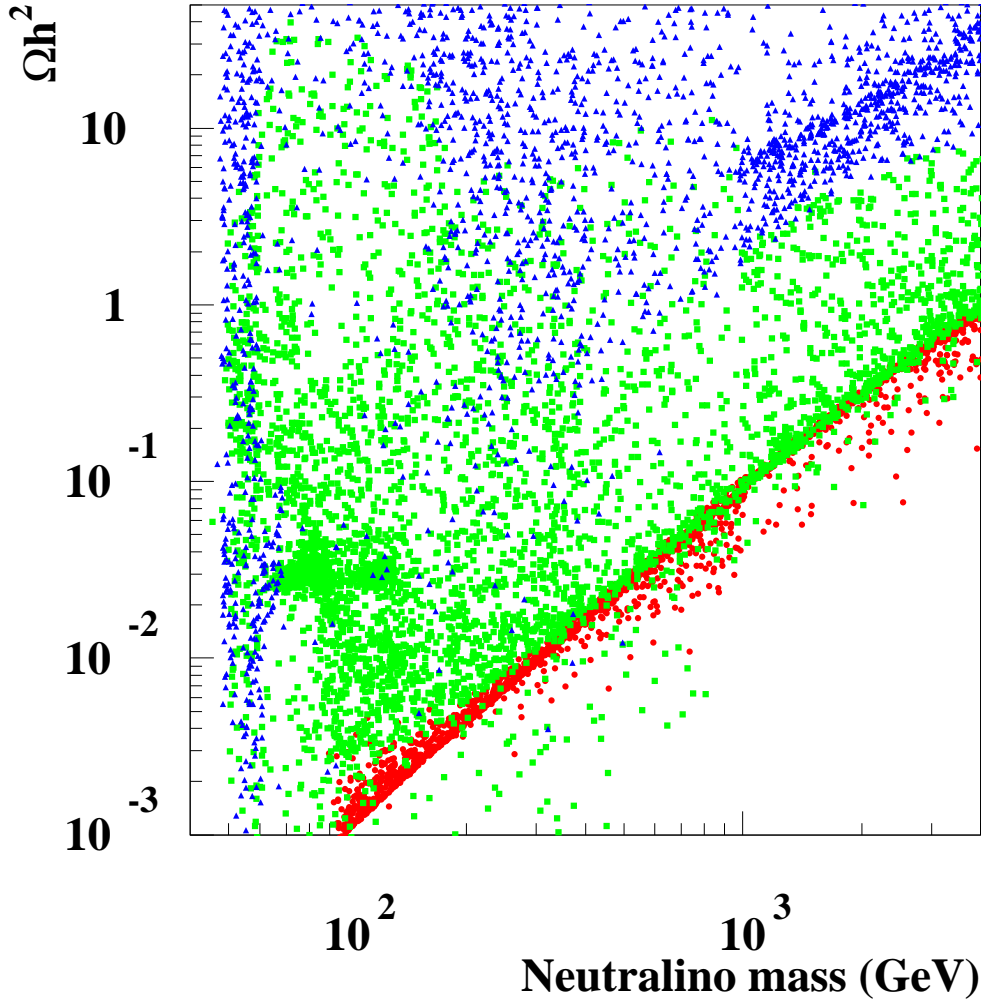


Figure 6. The computed relic density $\Omega_\chi h^2$ of the lightest neutralino versus mass in a large sampling of supersymmetric parameter space. The filled circles denote higgsino-like models with gaugino fraction $Z_g < 0.01$, squares are mixed models with $0.01 < Z_g < 0.99$ and triangles are gaugino models with $Z_g > 0.99$. For details of the calculation, see [135, 134] and references therein.

8.2. Other supersymmetric candidates

Although the neutralino is considered by most workers in the field to be the preferred supersymmetric dark matter candidate, we mention briefly here also some other options. One possibility is provided by the sneutrino, the supersymmetric partner of one of the neutrinos. This would give rise to a large coupling to ordinary matter (and also annihilation cross section) through Z boson exchange, and has therefore long been

thought to be disfavoured [116]. However, in non-minimal models these Z couplings may be suppressed, and there are versions which are still viable, although rather constrained [136].

If the axion exists, and if the underlying theory is supersymmetric, there should also exist a spin-1/2 partner, the axino. If this is the lightest supersymmetric particle and is in the multi-GeV mass range, it could compose the cold dark matter of the universe [137]. If it is lighter, it could act as mixed dark matter [138] with a non-thermal component arising from neutralino decay into axinos and perhaps mix with neutrinos if R -parity is violated [139].

A completely different type of supersymmetric dark matter candidate is provided by so-called Q-balls [140], non-topological solitons predicted to be present in many versions of the theory. These are produced in a non-thermal way and may have large lepton or baryon number. They could produce unusual ionization signals in neutrino telescopes, for example. However, the unknown properties of their precise formation mechanism means that their relic density may be far below the level of observability, and a value around the observationally favoured $\Omega_M \sim 0.3$ may seem fortuitous.

Of course, there remains the possibility of dark matter being non-supersymmetric WIMPs. However, for the general reasons explained in Section 3, the interaction cross sections should then be quite similar as for supersymmetric particles. Since, the rates in the MSSM are completely calculable once the supersymmetry parameters are fixed, these particles, in particular neutralinos, serve as important templates for reasonable dark matter candidates when it comes to designing experiments with the purpose of detecting dark matter WIMPs.

9. Detection methods for neutralino dark matter

The ideal situation would appear if supersymmetry were discovered at accelerators, so that direct measurements of the mass of the lightest supersymmetric particle, its couplings and other properties could be performed. This would give a way to check from very basic principle if this particle is a good dark matter candidate - if it is electrically neutral and has the appropriate mass and couplings to give the required relic density to provide $\Omega_M \sim 0.3$. So far, no signal of supersymmetry has been found at either LEP or Fermilab, but hopefully the situation may change as Fermilab's new Main Injector gets into operation. It may be, however, that one will have to wait for CERN's Large Hadron Collider to come into operation some time after 2005 before a signal of supersymmetry may be seen. (An indirect piece of evidence for supersymmetry would be the discovery of a Higgs particle below around 130 GeV. In the non-supersymmetric Standard Model the Higgs could be much heavier.)

The long time scale of designing and building new accelerators (and the possibility that the dark matter particles may be extremely heavy or otherwise difficult to produce and detect) means that it is certainly worthwhile to explore the possibility to detect the putative dark matter particles as they move in the Galactic halo. This can be done

directly in terrestrial detectors sensitive to the nuclear recoil and/or ionization caused by the passing wind of dark matter particles, or indirectly by detecting products of annihilations of dark matter particles such as gamma rays, antiprotons or positrons, in the Galactic halo or in the Earth or Sun (in which case neutrinos could give an indirect signal).

9.1. Direct searches of halo dark matter

As explained above, we use the neutralino of the MSSM as a template for an excellent dark matter candidate. If these neutralinos are indeed the CDM needed on galaxy scales and larger, there should be a substantial flux of these particles in the Milky Way halo. Since the interaction strength is essentially given by the same weak couplings as, e.g., for neutrinos there is a non-negligible chance of detecting them in low-background counting experiments [141]. Due to the large parameter space of MSSM, even with the simplifying assumptions above, there is a rather wide span of predictions for the event rate in detectors of various types. It is interesting, however, that the models giving the largest rates are already starting to be ruled out by present direct detection experiments [133, 142].

If we assume a local neutralino halo density of $\rho_\chi = \rho_\odot \sim 0.3 \text{ GeV/cm}^3$, and a typical galactic velocity of neutralinos of $v/c \sim 10^{-3}$, the flux of particles of mass 100 GeV at the location of a detector at the Earth is roughly $10^9 \text{ m}^{-2} \text{ s}^{-1}$. Although this may seem as a high flux, the interaction rate has to be quite small, since we saw in Section 3 that the correct magnitude of $\Omega_\chi \sim 0.3$ is only achieved if the annihilation cross section, and therefore by expected crossing symmetry also the scattering cross section, is of weak interaction strength.

The rate for direct detection of galactic neutralinos, integrated over deposited energy assuming no energy threshold, is

$$R = \sum_i N_i n_\chi \langle \sigma_{i\chi} v \rangle, \quad (49)$$

where N_i is the number of nuclei of species i in the detector, n_χ is the local galactic neutralino number density, $\sigma_{i\chi}$ is the neutralino-nucleus elastic cross section, and the angular brackets denote an average over v , the neutralino speed relative to the detector.

The most important direct detection process is elastic scattering on nuclei, although inelastic processes [143, 144, 145] and scattering on electrons [146] have also been suggested in the literature. Since neutralinos are Majorana particles, there exist selection rules which dictate the form of the effective interaction Lagrangian. For instance, since a Majorana fermion can carry no non-zero conserved additive quantum number (due to the requirement that they be self-charge-conjugate fields), the vector current vanishes identically. The most important non-vanishing currents are then the scalar-scalar coupling giving a spin-independent effective interaction, and the axial-axial current which couples proportionally to the spin of the nucleus:

$$\mathcal{L}_{\text{eff}} = f_{SI} (\bar{\chi}\chi) (\bar{N}N) + f_{SD} (\bar{\chi}\gamma^\mu\gamma^5\chi) (\bar{N}\gamma_\mu\gamma^5N). \quad (50)$$

Usually, it is the spin-independent interaction that gives the most important contribution in realistic target materials (such as Na, Cs, Ge, I, or Xe), due to the enhancement caused by the coherence of all nucleons in the target nucleus.

The neutralino-nucleus elastic cross section can be written as

$$\sigma_{i\chi} = \frac{1}{4\pi v^2} \int_0^{4m_{i\chi}^2 v^2} dq^2 G_{i\chi}^2(q^2), \quad (51)$$

where $m_{i\chi}$ is the neutralino-nucleus reduced mass, q is the momentum transfer and $G_{i\chi}(q^2)$ is the effective neutralino-nucleus vertex. One may write

$$G_{i\chi}^2(q^2) = A_i^2 F_{SI}^2(q^2) G_{SI}^2 + 4\lambda_i^2 J(J+1) F_{SD}^2(q^2) G_{SD}^2, \quad (52)$$

which shows the coherent enhancement factor A_i^2 for the spin-independent cross section. A reasonable approximation for the gaussian scalar and axial nuclear form factors is [147]

$$F_{SI}(q^2) = F_{SD}(q^2) = \exp(-q^2 R_i^2 / 6\hbar^2), \quad (53)$$

$$R_i = (0.3 + 0.89A_i^{1/3}) \text{ fm}, \quad (54)$$

which gives good approximation to the integrated detection rate [148] (but is less accurate for the differential rate [149]). Here λ_i is related to the average spin of the nucleons making up the nucleus. For the relation between G_{SI} , G_{SD} and f_{SI} , f_{SD} as well as a discussion of the several Feynman diagrams which contribute to these couplings, see e.g. [133, 150, 151]. One should be aware that both the choice of nuclear form factors and effective neutralino-nucleon vertices as well as the numerical values adopted for the nucleon matrix elements are at best approximate. A more sophisticated treatment (see discussion and references in [10]) would, however, change the values by much less than the spread due to the unknown supersymmetric parameters.

For a target consisting of N_i nuclei the differential scattering rate per unit time and unit recoil energy E_R is given by

$$S_0(E_R) = \frac{dR}{dE_R} = N_i \frac{\rho_\chi}{m_\chi} \int d^3v f(\vec{v}) v \frac{d\sigma_{i\chi}}{dE_R}(v, E_R). \quad (55)$$

The nuclear recoil energy E_R is given by

$$E_R = \frac{m_{i\chi}^2 v^2 (1 - \cos \theta^*)}{m_i} \quad (56)$$

where θ^* is the scattering angle in the center of mass frame. The range and slope of the recoil energy spectrum is essentially given by non-relativistic kinematics. For a low-mass χ , the spectrum is steeply falling with E_R ; interaction with a high-mass χ gives a flatter spectrum with higher cutoff in E_R .

The total predicted rate integrated over recoil energy above a given generally (detector-dependent) threshold can be compared with upper limits coming from various direct detection experiments. In this way, limits on the χ -nucleon cross section have been obtained as a function of the mass m_χ [152]. The cross section on neutrons is usually very similar to that on protons, so in general only the latter is displayed. In Fig. 7 is shown a scatter plot of the spin-independent neutralino-proton cross sections as a function of

neutralino mass predicted in an extensive scan of the MSSM parameter space. This is the same scan as that used in [134] (see also references therein) except for updated LEP bounds: $m_{\chi^\pm} > 95$ GeV, $m_{H_2} > 100$ GeV. These latter bounds are simplified and somewhat overconstraining. The actual bounds depend on other parameters such as $\tan\beta$ and the detailed decay modes. In this figure, only the range $0.1 < \Omega_\chi h^2 < 0.2$ has been selected, as this is the favoured range for CDM as discussed before. This more lower bound is more restrictive than usually employed ($\Omega h^2 > 0.025$), but also more strongly motivated by cosmology. It has the effect of excluding some model with large scattering cross sections. Also shown are the present experimental upper bounds as well as the region consistent with the possible DAMA signal discussed below. A major step forward is expected within a couple of years. For example, the CDMS experiment will be moved from a shallow Stanford site to the well-shielded Soudan mine. This together with a larger detector mass and other improvements will enable a thorough search well beyond the range suggested by DAMA. Also in Europe there are several ambitious endeavours underway, such as the GENIUS detector [161], CRESST2 [162] and UKDMC [163]. As can be seen in the Figure, some of these experiments will start to probe interesting regions of neutralino dark matter.

The rate in Eq. (55) is strongly dependent on the velocity v of the neutralino with respect to the target nucleus. Therefore, as explained in Section 6.1 an annual modulation of the counting rate is in principle possible, due to the motion of the Earth around the Sun [71]. One can thus write

$$S(E_R, t) = S_0(E_R) + S_m(E_R) \cos[\omega(t - t_0)], \quad (57)$$

where $\omega = 2\pi/365$ days⁻¹. Starting to count time in days from January 1st, the phase is $t_0 = 153$ days since the maximal signal occurs when the direction of motion of the Earth around the Sun and the Sun around the galactic center coincide maximally, which happens on June 2nd every year [71]. Similarly, the counting rate is expected to be the lowest December 2nd every year. Here $S_0(E_r)$ is the average differential scattering rate in Eq. (55) and $S_m(E_R)$ is the modulation amplitude of the rate. The relative size of $S_m(E_R)$ and $S_0(E_R)$ depends on the target and neutralino mass as well as on E_R . Typically $S_m(E_R)$ is of the order of a few percent of $S_0(E_R)$, but may approach 10 % for small m_χ (below, say, 50 GeV) and small E_R (below some 10 keV).

Since the basic couplings in the MSSM are between neutralinos and quarks, there are uncertainties related to the hadronic physics step which relates quarks/gluons with nucleons as well the step from nucleons to nuclei. These uncertainties are substantial, and can plague all estimates of scattering rates by at least a factor of 2, maybe even by an order of magnitude [153]. The largest rates, which as first shown in [133] could be already ruled out by current experiments, are generally obtained for mixed neutralinos, i.e. with Z_g neither very near 0 nor very near 1, and for relatively light Higgs masses (since Higgs bosons mediate a scalar, spin-independent exchange interaction). This means that the LEP bounds on the supersymmetric Higgs particle masses put relevant constraints on the predicted detection rates.

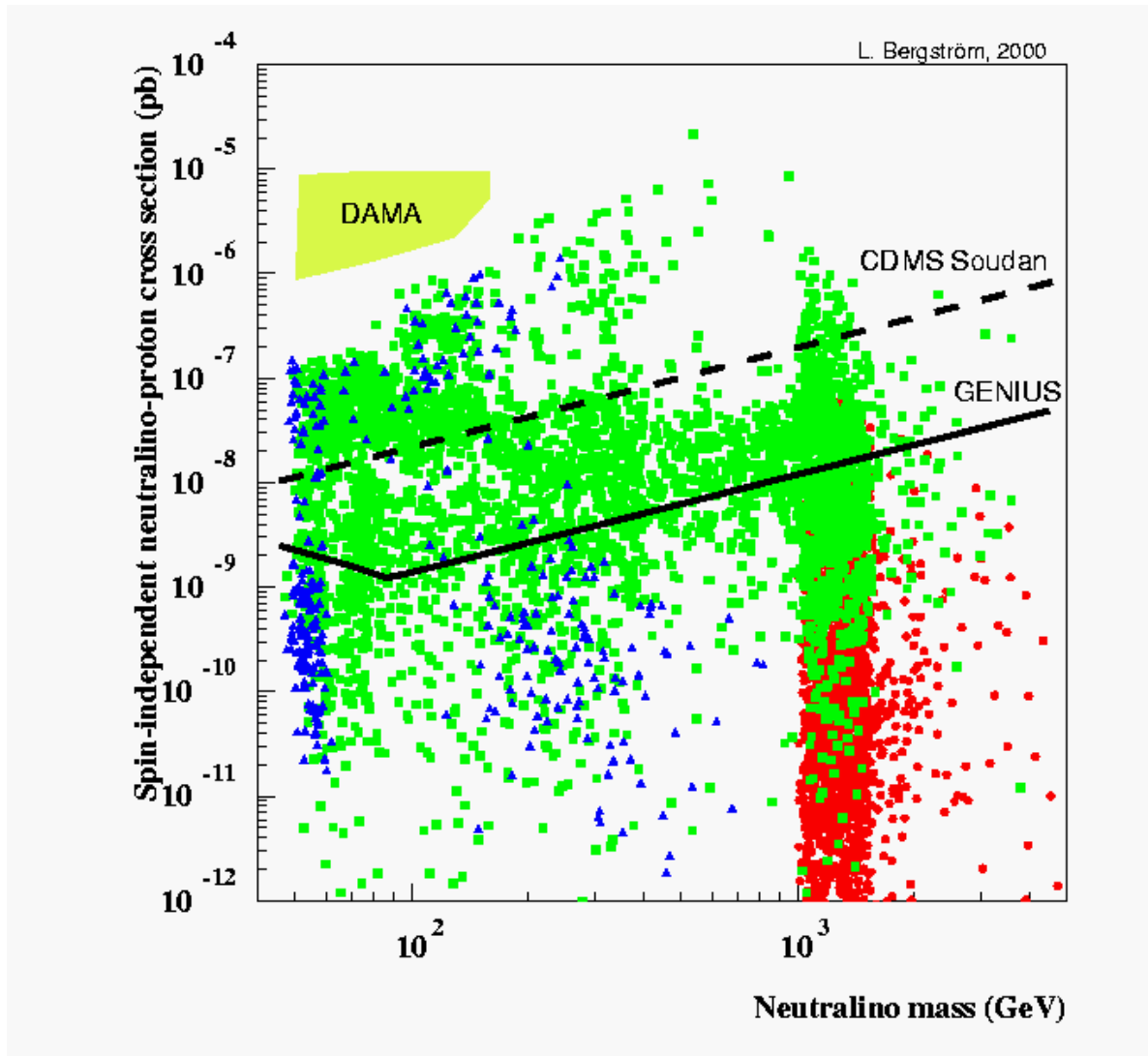


Figure 7. The neutralino-proton cross section versus mass for a large scan in supersymmetric parameter space fulfilling $0.1 < \Omega_\chi h^2 < 0.2$, $m_{\chi^\pm} > 95$ GeV and $m_{H_2^0} > 100$ GeV (the cross section on neutrons is very similar). The filled circles denote higgsino-like models with gaugino fraction $Z_g < 0.01$, squares are mixed models with $0.01 < Z_g < 0.99$ and triangles are gaugino models with $Z_g > 0.99$. The region consistent with the claimed DAMA signal [154] is indicated. The approximate expected sensitivity curves of the proposed CDMS-Soudan and GENIUS experiments are also shown.

The experimental situation is becoming interesting as several direct detection experiments after many years of continuing sophistication are starting to probe interesting parts of the parameter space of the MSSM, given reasonable, central values of the astrophysical and nuclear physics parameters. Perhaps most striking is the evidence for an annual modulation effect claimed to be seen in the NaI experiment DAMA [154]. This has been interpreted as possibly being due to a neutralino of the MSSM [155, 156]. It seems premature, however, to draw strong conclusions from this experiment alone.

Besides some cloudy experimental issues [157, 158], the implied scattering rate seems somewhat too high for the MSSM, given the recent strong Higgs mass bounds from LEP operating above 200 GeV (especially if one wants $\Omega_\chi \gtrsim 0.2$), unless one really stretches the astrophysical [159, 160] and nuclear physics quantities [153]. This is seen in Fig. 7, where the DAMA region is not populated by any points. The main reason for this is the Ω cut. If the lower bound is relaxed to $\Omega_\chi h^2 > 0.025$, some models would appear in the DAMA region. It is probably also possible, but not very attractive, to find points with higher rates by making special samplings in parameter space designed just to find such high rates. Clearly, more sensitive experiments are needed to settle this issue.

Many of the present day detectors are severely hampered by a large background of various types of ambient radioactivity or cosmic-ray induced activity (neutrons are a particularly severe problem since they may produce recoils which are very similar to the expected signal). A great improvement in sensitivity would be acquired if one could use directional information about the recoils [164]. There are some very interesting developments also along this line [165], but a full-scale detector is yet to be built. Direction-sensitive detectors would have an even bigger advantage over pure counting experiments if the dark matter velocity distribution is less trivial than the commonly assumed maxwellian, as has been recently suggested [166, 167].

9.2. Indirect searches

Besides these possibilities of direct detection of supersymmetric dark matter (with even a weak indication of the existence of a signal [154]), one also has the possibility of indirect detection through neutralino annihilation in the galactic halo. This is becoming a promising method thanks to very powerful new detectors for cosmic gamma rays and neutrinos planned and under construction.

There has been a balloon-borne detection experiment [168], with increased sensitivity to eventual positrons from neutralino annihilation, where an excess of positrons over that expected from ordinary sources was found. However, since there are many other possibilities to create positrons by astrophysical sources, e.g., near the centre of the Milky Way, the interpretation is not yet conclusive. Also, another measurement does not confirm this excess [169].

Antiprotons, \bar{p} , from neutralino annihilations were long hoped to give a useful signal [170], and there have been several balloon-borne experiments [171, 172] performed and a very ambitious space experiment, AMS, to search for antimatter is under way [173]. For kinematical reasons, antiprotons created by pair-production in cosmic ray collisions with interstellar gas and dust are born with relatively high energy, whereas antiprotons from neutralino annihilation populate also the sub-100 MeV energy band.

However, it was found recently [174, 175] that the cosmic-ray induced antiprotons may populate also the low-energy region to a greater extent than previously thought, making the extraction of an eventual supersymmetric signal much more difficult. There are basically three effects which cause this problem. First, helium and other heavier

elements in the interstellar medium give an antiproton yield at lower energy than hydrogen, since the centre of mass system is kinematically closer to the galactic rest frame. Secondly, antiprotons may be produced at incident and outgoing nominal kinetic energies below the threshold energies valid for proton-proton collisions, due to collective nuclear effects. And, thirdly, secondary elastic and inelastic interactions of produced antiprotons give a “tertiary” \bar{p} component at lower kinetic energy.

Another problem that plagues estimates of the signal strength of both positrons and antiprotons is the uncertainty of the galactic propagation model and solar wind modulation.

Even allowing for large such systematic effects, the measured antiproton flux gives, however, rather stringent limits on MSSM models with the highest annihilation rates. One can also use the experimental upper limits to bound from below the lifetime of hypothetical R -parity violating decaying neutralinos [176]. There may in some scenarios with a clumpy halo (which enhances the annihilation rate) be a possibility to detect heavy neutralinos through spectral features above several GeV [177].

A very rare process in proton-proton collisions, antideuteron production, may be less rare in neutralino annihilation [178]. However, the fluxes are so small that the possibility of detection seems marginal even in the AMS experiment.

9.3. Indirect detection by gamma rays from the halo

With the problem of a lack of clear signature of positrons and antiprotons, one would expect that the situation of gamma rays and neutrinos is similar, if they only arise from secondary decays in the annihilation process. For instance, the gamma ray spectrum arising from the fragmentation of fermion and gauge boson final states is quite featureless and gives the bulk of the gamma rays at low energy where the cosmic gamma ray background is severe. However, an advantage is the directional information that photons carry in contrast to charged particles which random walk through the magnetic fields of the Galaxy [179].

9.3.1. Gamma ray lines An early idea was to look for a spectral feature, a line, in the radiative annihilation process to a charm-anticharm bound state $\chi\chi \rightarrow (\bar{c}c)_{\text{bound}} + \gamma$ [180]. However, as the experimental lower bound on the lightest neutralino became higher it was shown that form factor suppression rapidly makes this process unfeasible [181]. The surprising discovery was made that the loop-induced annihilations $\chi\chi \rightarrow \gamma\gamma$ [181, 182] and $\chi\chi \rightarrow Z\gamma$ [183] do not suffer at all from any form factor suppression (this was subsequently shown to be related to the famous triangle anomaly of quantum field theory [184]).

The rates of these processes are difficult to estimate because of uncertainties in the supersymmetric parameters, cross sections and halo density profile. However, in contrast to the other proposed detection methods they have the virtue of giving very distinct, “smoking gun” signals of monoenergetic photons with energy $E_\gamma = m_\chi$ (for

$\chi\chi \rightarrow \gamma\gamma$) or $E_\gamma = m_\chi(1 - m_Z^2/4m_\chi^2)$ (for $\chi\chi \rightarrow Z\gamma$) emanating from annihilations in the halo.

The detection probability of a gamma ray signal, either continuous or line, will of course depend sensitively on the density profile of the dark matter halo. To illustrate this point, let us consider the characteristic angular dependence of the gamma-ray line intensity from neutralino annihilation $\chi\chi \rightarrow \gamma\gamma$ in the galactic halo. Annihilation of neutralinos in an isothermal halo with core radius a leads to a gamma-ray flux along the line-of-sight direction \hat{n} of

$$\frac{d\mathcal{F}}{d\Omega}(\hat{n}) \simeq (2 \times 10^{-13} \text{cm}^{-2} \text{s}^{-1} \text{sr}^{-1}) \times \left(\frac{\sigma_{\gamma\gamma} v}{10^{-29} \text{cm}^{-3} \text{s}^{-1}} \right) \left(\frac{\rho_\chi}{0.3 \text{GeV cm}^{-3}} \right)^2 \left(\frac{100 \text{GeV}}{m_\chi} \right)^2 \left(\frac{R}{8.5 \text{kpc}} \right) J(\hat{n}) \quad (58)$$

where $\sigma_{\gamma\gamma} v$ is the annihilation rate, ρ_χ is the local neutralino halo density and R is the distance to the galactic center. The integral $J(\hat{n})$ is given by

$$J(\hat{n}) = \frac{1}{R\rho_\chi^2} \int_{\text{line-of-sight}} \rho^2(\ell) d\ell(\hat{n}), \quad (59)$$

and is evidently very sensitive to local density variations along the line-of-sight path of integration. In the case of a smooth halo, its value ranges from a few at high galactic latitudes to several thousand for a small angle average towards the galactic center in the NFW model [68].

We remind of the fact that since the neutralino velocities in the halo are of the order of 10^{-3} of the velocity of light, the annihilation can be considered to be at rest. The resulting gamma ray spectrum is a line at $E_\gamma = m_\chi$ of relative linewidth 10^{-3} which in favourable cases will stand out against background.

The calculation of the $\chi\chi \rightarrow \gamma\gamma$ cross section is technically quite involved with a large number of loop diagrams contributing. In fact, only very recently a full calculation in the MSSM was performed [185]. Since the different contributions all have to be added coherently, there may be cancellations or enhancements, depending on the supersymmetric parameters. The process $\chi\chi \rightarrow Z\gamma$ is treated analogously and has a similar rate [183].

An important contribution, especially for neutralinos that contain a fair fraction of a higgsino component, is from virtual W^+W^- intermediate states. This is true both for the $\gamma\gamma$ and $Z\gamma$ final state for very massive neutralinos [183]. In fact, thanks to the effects of coannihilations [124], neutralinos as heavy as several TeV are allowed without giving a too large Ω . These extremely heavy dark matter candidates (which, however, would require quite a degree of finetuning in most supersymmetric models) are predominantly higgsinos and have a remarkably large branching ratio into the loop-induced $\gamma\gamma$ and $Z\gamma$ final states (the sum of these can be as large as 30%). If there would exist such heavy, stable neutralinos, the gamma ray line annihilation process may be the only one which could reveal their existence in the foreseeable future (since not even LHC would be sensitive to supersymmetry if the lightest supersymmetric particle weighs several

TeV)].

To compute $J(\hat{n})$ in Eq. (59), a model of the dark matter halo has to be chosen, as discussed in Section 6. The universal halo profile found in simulations by Navarro, Frenk and White [188] has a rather significant enhancement $\propto 1/r$ near the halo centre. (In fact, as was seen in Section 6, other simulations give even steeper central halo profiles.) If applicable to the Milky Way, this would lead to a much enhanced annihilation rate towards the galactic centre, and also to a very characteristic angular dependence of the line signal. This would be very beneficial when discriminating against the extragalactic γ ray background, and Air Cherenkov Telescopes (ACTs) would be eminently suited to look for these signals since they have an angular acceptance which is well matched to the angular size of the Galactic central region where a cusp is likely to be. However, to search for lines the energy resolution has to be at the 10 – 20 % level, which is difficult but possible with present-day technology.

Space-borne gamma ray detectors, like the projected GLAST satellite [189], have a much smaller area (on the order of 1 m² instead of 10⁴ – 10⁵ m² for ACTs), but a correspondingly larger angular acceptance so that the integrated sensitivity is in fact similar. This is at least true if the Galactic center does not have a very large dark matter density enhancement which would favour ACTs. The total rate expected in GLAST can be computed with much less uncertainty because of the angular integration. Directional information is obtained and can be used to discriminate against the diffuse extragalactic background. A line signal can be searched for with high precision, since the energy resolution of GLAST will be at the few percent level. In Fig. 8 is shown the potential for GLAST assuming a NFW profile and an exposure time of 4 years. As can be seen, there is a region below around 250 GeV where these processes are observable for the models with the highest rates.

In Fig. 9 is shown the corresponding gamma ray line flux in an ACT assuming an effective value of 10³ for the average of $J(\hat{n})$ over the 10⁻³ steradians that typically an ACT would cover. (See [68] for details.)

It can be seen that the models which give the highest rates should also be within reach of the new generation of ACTs presently being constructed. These will have an effective area of almost 10⁵ m², a threshold of some tens of GeV and an energy resolution approaching 10 %. As seen in Fig. 9, even TeV masses could be accessible through this method. At the low m_χ end, also a smaller area detector with better energy resolution and wider angular acceptance such as the proposed GLAST satellite could reach discovery potential. It is important to note that direct detection as discussed in Section 9.1 and indirect detection through gamma ray lines are complementary to each other. This is illustrated in Fig. 10, where $\sigma_{\gamma\gamma}v$ is displayed against $\sigma_{p\chi}$ for our sampling of the MSSM. As can be seen, the two types of process are nicely complementing each

|| Recently, there has been some interest in TeV neutralinos due to a claim of a possible structure in existing data [186]. It seems, however, that this claim was based on an erroneous estimate of the acceptance of the experiments [187]. Also, the purported rate is at least 3 or 4 orders of magnitude larger than what can be obtained in supersymmetric models [185].

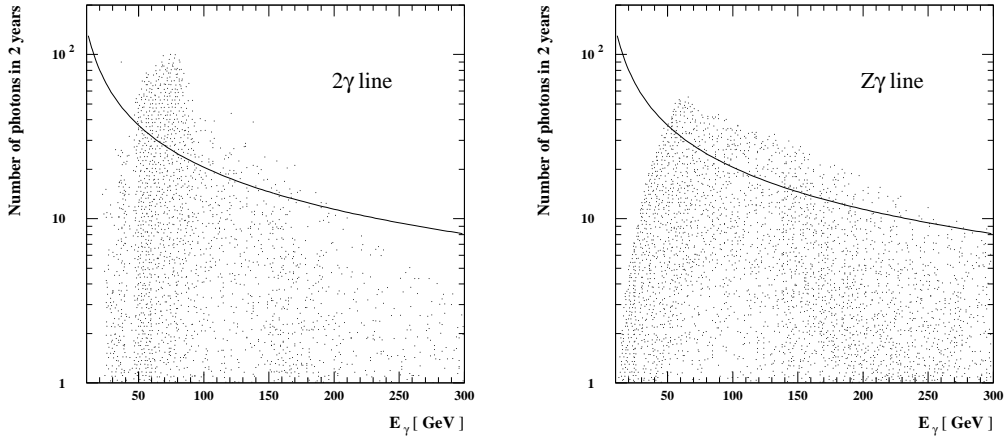


Figure 8. Results for the gamma ray line flux from $\chi\chi \rightarrow \gamma\gamma$ (left) and $\chi\chi \rightarrow Z\gamma$ (right) in an extensive scan of supersymmetric parameter space in the MSSM [68]. Shown is the number of events versus photon energy in the GLAST space-borne gamma ray detector during a 2-year exposure. The halo profile of [188] for the dark matter has been assumed. The estimated sensitivity of GLAST is shown as the solid line, taking the diffuse gamma-ray background into account.

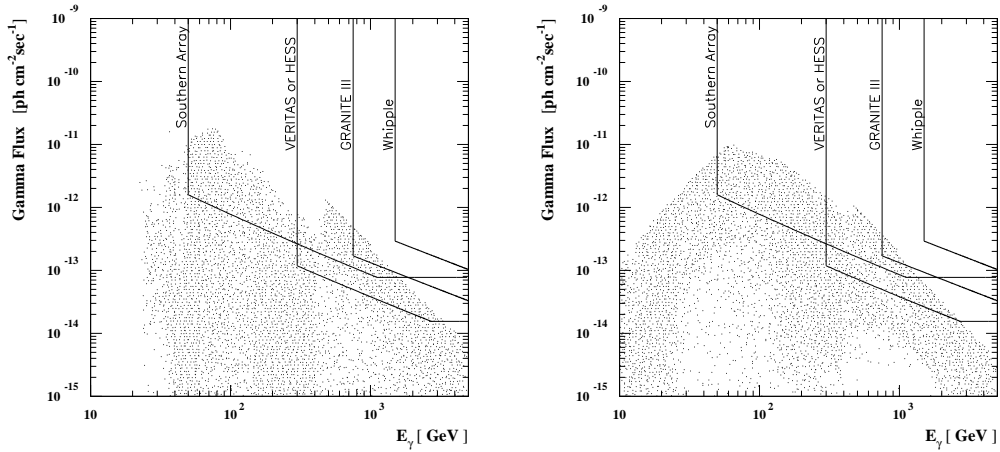


Figure 9. Results for the gamma ray line flux from $\chi\chi \rightarrow \gamma\gamma$ (left) and $\chi\chi \rightarrow Z\gamma$ (right) in an extensive scan of supersymmetric parameter space in the MSSM [68]. Shown is the number of events versus photon energy in an Air Cherenkov Telescope of area $5 \cdot 10^4 \text{ m}^2$ viewing the galactic centre for one year. The halo profile of [188] for the dark matter has been assumed.

other. In particular, models with m_χ larger than 400 GeV which generally have a small direct detection rate usually have a substantial annihilation rate in the $\gamma\gamma$ mode.

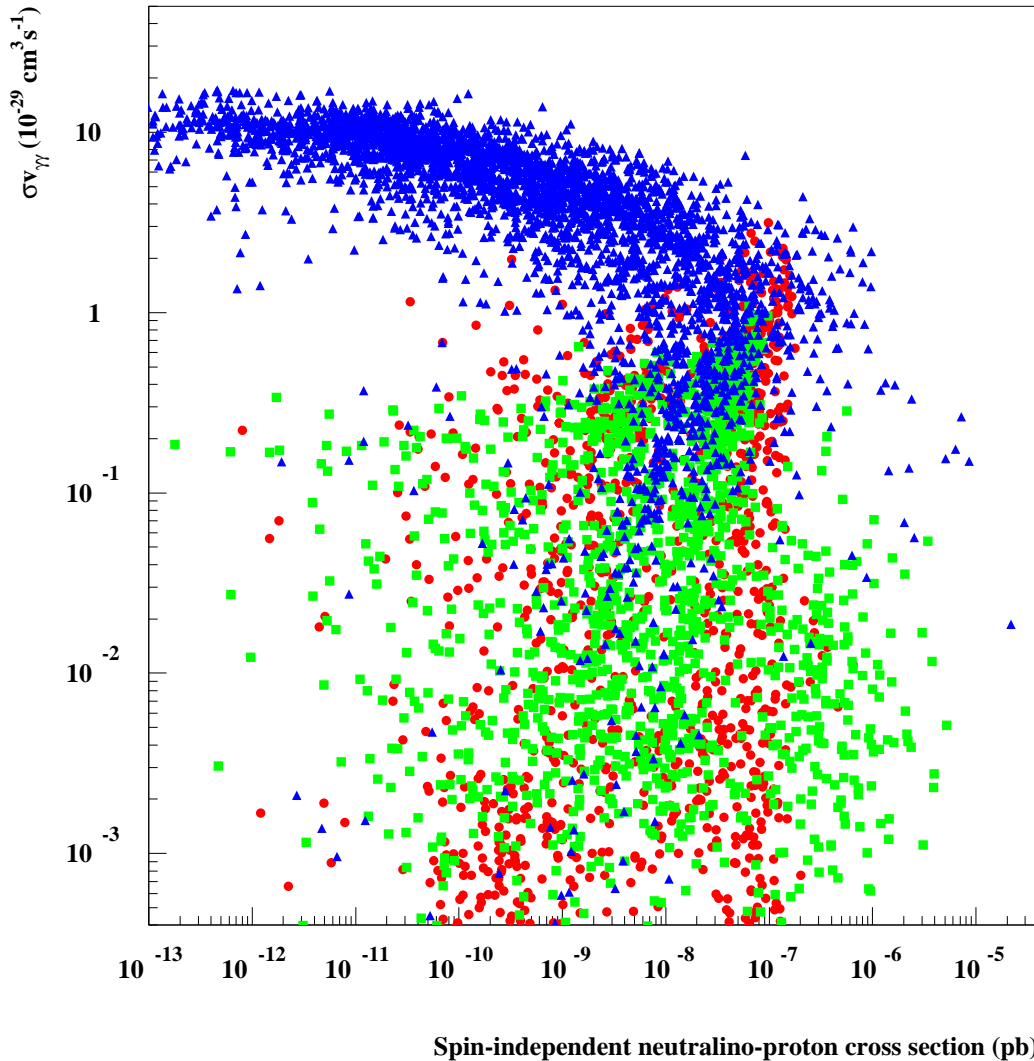


Figure 10. Comparison of direct/indirect detection strength for the full sample of points in MSSM parameter space. On the vertical axis is plotted the value of $\sigma_{\gamma\gamma}v$ (in units of $10^{-29} \text{ cm}^3 \text{ s}^{-1}$), and on the horizontal axis is shown the neutralino-proton cross section in picobarns. The filled circles denote models with $m_\chi < 100 \text{ GeV}$, squares have $100 \text{ GeV} < m_\chi < 400 \text{ GeV}$ and triangles are models with $m_\chi > 400 \text{ GeV}$. The large spread of values illustrates the complementarity of the processes. In particular, it is seen how the $\gamma\gamma$ process has a large rate for the very heavy (higgsino-like) neutralinos which have a small scattering cross section. The requirements $m_{\chi^\pm} > 95 \text{ GeV}$, $m_{H_2} > 100 \text{ GeV}$, $0.1 < \Omega_\chi h^2 < 0.2$ have been imposed.

9.3.2. Indirect detection through neutrinos The density of neutralinos in the halo is not large enough to give a measurable flux of secondary neutrinos, unless the dark matter halo is very clumpy [135]. In particular, the central Galactic black hole may have interacted with the dissipationless dark matter of the halo so that a spike of

very high dark matter density may exist right at the Galactic centre [190]. However, the existence of these different forms of density enhancements are very uncertain and depend extremely sensitively on presently completely unknown aspects of the formation history of the Milky Way.

More model-independent predictions (where essentially only the relatively well-determined local halo dark matter density is of importance) can be made for neutrinos from the centre of the Sun or Earth, where neutralinos may have been gravitationally trapped and therefore their density enhanced. As they annihilate, many of the possible final states (in particular, $\tau^+\tau^-$ lepton pairs, heavy quark-antiquark pairs and, if kinematically allowed, $W^\pm H^\mp$, $Z^0 H_i^0$, W^+W^- or $Z^0 Z^0$ pairs) give after decays and perhaps hadronization energetic neutrinos which will propagate out from the interior of the Sun or Earth. (For neutrinos from the Sun, energy loss of the hadrons in the solar medium and the energy loss of neutrinos have to be considered [191, 192]). In particular, the muon neutrinos are useful for indirect detection of neutralino annihilation processes, since muons have a quite long range in a suitable detector medium like ice or water. Therefore they can be detected through their Cherenkov radiation after having been produced at or near the detector, through the action of a charged current weak interaction $\nu_\mu + A \rightarrow \mu + X$.

Detection of neutralino annihilation into neutrinos is one of the most promising indirect detection methods, and will be subject to extensive experimental investigations in view of the new neutrino telescopes (AMANDA, IceCube, Baikal, NESTOR, ANTARES) planned or under construction [193]. The advantage shared with gamma rays is that neutrinos keep their original direction. A high-energy neutrino signal in the direction of the centre of the Sun or Earth is therefore an excellent experimental signature which may stand up against the background of neutrinos generated by cosmic-ray interactions in the Earth's atmosphere.

The differential neutrino flux from neutralino annihilation is

$$\frac{dN_\nu}{dE_\nu} = \frac{\Gamma_A}{4\pi D^2} \sum_f B_\chi^f \frac{dN_\nu^f}{dE_\nu} \quad (60)$$

where Γ_A is the annihilation rate, D is the distance of the detector from the source (the central region of the Earth or the Sun), f is the neutralino pair annihilation final states, and B_χ^f are the branching ratios into the final state f . dN_ν^f/dE_ν are the energy distributions of neutrinos generated by the final state f . Detailed calculations of these spectra can be made using Monte Carlo methods [194, 192, 195].

The neutrino-induced muon flux may be detected in a neutrino telescope by measuring the muons that come from the direction of the centre of the Sun or Earth. For a shallow detector, this usually has to be done in the case of the Sun by looking (as always the case for the Earth) at upward-going muons, since there is a huge background of downward-going muons created by cosmic-ray interactions in the atmosphere. There is always in addition a more isotropic background coming from muon neutrinos created on the other side of the Earth in such cosmic-ray events (and also from cosmic-ray

interactions in the outer regions of the Sun). The flux of muons at the detector is given by

$$\frac{dN_\mu}{dE_\mu} = N_A \int_{E_\mu^{\text{th}}}^\infty dE_\nu \int_0^\infty d\lambda \int_{E_\mu}^{E_\nu} dE'_\mu P(E_\mu, E'_\mu; \lambda) \frac{d\sigma_\nu(E_\nu, E'_\mu)}{dE'_\mu} \frac{dN_\nu}{dE_\nu}, \quad (61)$$

where λ is the muon range in the medium (ice or water for the large detectors in the ocean or at the South Pole, or rock which surrounds the smaller underground detectors), $d\sigma_\nu(E_\nu, E'_\mu)/dE'_\mu$ is the weak interaction cross section for production of a muon of energy E'_μ from a parent neutrino of energy E_ν , and $P(E_\mu, E'_\mu; \lambda)$ is the probability for a muon of initial energy E'_μ to have a final energy E_μ after passing a path-length λ inside the detector medium. E_μ^{th} is the detector threshold energy, which for “small” neutrino telescopes like Baksan, MACRO and Super-Kamiokande is around 1 GeV. Large area neutrino telescopes in the ocean or in Antarctic ice typically have thresholds of the order of tens of GeV, which makes them sensitive mainly to heavy neutralinos (above 100 GeV) [196]. Convenient approximation formulas relating the observable muon flux to the neutrino flux at a given energy can be found in [197].

The integrand in Eq. (61) is weighted towards high neutrino energies, both because the cross section σ_ν rises approximately linearly with energy and because the average muon energy, and therefore the range λ , also grow approximately linearly with E_ν . Therefore, final states which give a hard neutrino spectrum (such as heavy quarks, τ leptons and W or Z bosons) are usually more important than the soft spectrum arising from light quarks and gluons.

The rate of change of the number of neutralinos N_χ in the Sun or Earth is governed by the equation

$$\dot{N}_\chi = C_C - C_A N_\chi^2 \quad (62)$$

where C_C is the capture rate and C_A is related to the annihilation rate Γ_A , $\Gamma_A = C_A N_\chi^2$. This has the solution

$$\Gamma_A = \frac{C_C}{2} \tanh^2 \left(\frac{t}{\tau} \right), \quad (63)$$

where the equilibration time scale $\tau = 1/\sqrt{C_C C_A}$. In most cases for the Sun, and in the cases of observable fluxes for the Earth, τ is much smaller than a few billion years, and therefore equilibrium is often a good approximation ($\dot{N}_\chi = 0$ in Eq. (62)). This means that it is the capture rate which is the important quantity that determines the neutrino flux.

The capture rate induced by scalar (spin-independent) interactions between the neutralinos and the nuclei in the interior of the Earth or Sun is the most difficult one to compute, since it depends sensitively on Higgs mass, form factors, and other poorly known quantities. However, this spin-independent capture rate calculation is the same as for direct detection treated in Section 9.1. Therefore, there is a strong correlation between the neutrino flux expected from the Earth (which is mainly composed of spinless nuclei) and the signal predicted in direct detection experiments [196, 198]. It seems

that even the large (kilometer-scale) neutrino telescopes planned will not be competitive with the next generation of direct detection experiments when it comes to detecting neutralino dark matter, searching for annihilations from the Earth. However, the situation concerning the Sun is more favourable. Due to the low counting rates for the spin-dependent interactions in terrestrial detectors, high-energy neutrinos from the Sun constitute a competitive and complementary neutralino dark matter search. Of course, even if a neutralino is found through direct detection, it will be extremely important to confirm its identity and investigate its properties through indirect detection. In particular, the mass can be determined with reasonable accuracy by looking at the angular distribution of the detected muons [199, 200].

For the the Sun, dominated by hydrogen, the axial (spin-dependent) cross section is important and relatively easy to compute. A good approximation is given by [10]

$$\frac{C_{\odot}^{\text{sd}}}{(1.3 \cdot 10^{23} \text{ s}^{-1})} = \left(\frac{\rho_{\chi}}{0.3 \text{ GeV cm}^{-3}} \right) \left(\frac{100 \text{ GeV}}{m_{\chi}} \right) \left(\frac{\sigma_{p\chi}^{\text{sd}}}{10^{-40} \text{ cm}^2} \right) \left(\frac{270 \text{ km/s}}{\bar{v}} \right) \quad (64)$$

where $\sigma_{p\chi}^{\text{sd}}$ is the cross section for neutralino-proton elastic scattering via the axial-vector interaction, \bar{v} is the dark-matter velocity dispersion, and ρ_{χ} is the local dark matter mass. The capture rate in the Earth is dominated by scalar interactions, where there may be kinematic and other enhancements, in particular if the mass of the neutralino almost matches one of the heavy elements in the Earth. For this case, a more detailed analysis is called for, but convenient approximations are available [10]. In fact, also for the Sun the spin-dependent contribution can be important, in particular iron may contribute non-negligibly.

To illustrate the potential of neutrino telescopes for discovery of dark matter through neutrinos from the Earth or Sun, we present the results of a full calculation [196] in Fig. 11. The present experimental upper limits are of the order of a few thousand muon events per square kilometer and year (both for the Sun and the Earth), and the irreducible background from the cosmic rays producing neutrinos in the Sun's atmosphere is of the order of 20 (both the current limits and this background are only weakly dependent on neutralino mass, see [196]).

In Fig. 11 it can be seen that a neutrino telescope of area around 1 km², which is a size currently being discussed, would have discovery potential for a range of supersymmetric models.

It has recently been realized that even a small deviation from the usually assumed Maxwellian velocity distribution of neutralinos in the local part of the halo can have a large effect on the indirect detection rates from the Earth [134]. In particular, neutralinos which have scattered once by the Sun (going in Keplerian orbits through the outer layers of the Sun) may have their orbits perturbed by the large planets and will make up a new population in phase space with velocities close to the Earths orbital velocity around the Sun (but mainly going in nearly radial orbits). This low-velocity population

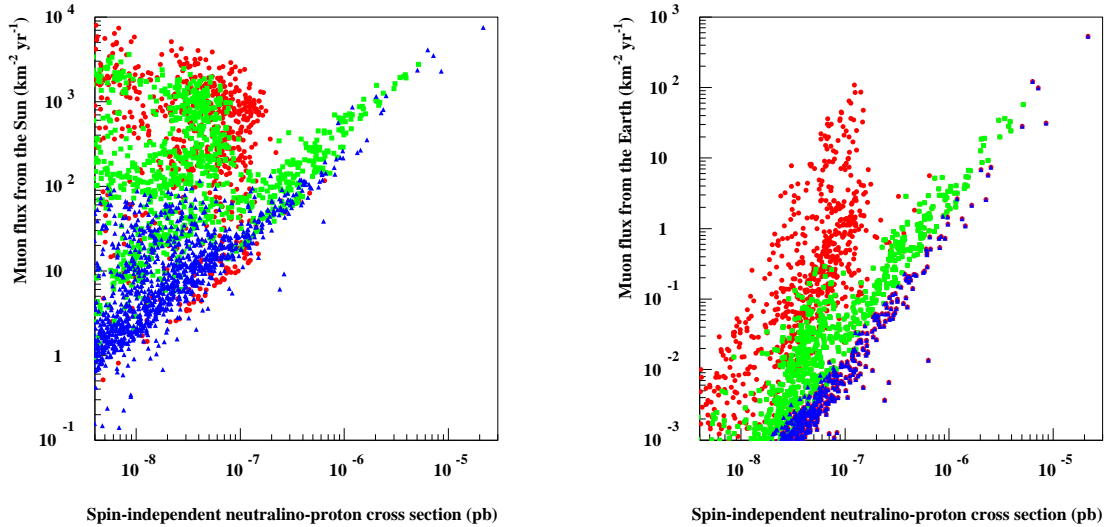


Figure 11. The predicted muon rates from neutralino annihilations in the Sun (left-hand figure) and in the Earth (right-hand figure) versus the neutralino-proton scattering cross section. A muon detection threshold of 1 GeV has been assumed. The requirements $m_{\chi_{\pm}} > 95$ GeV, $m_{H_2} > 100$ GeV, $0.1 < \Omega_{\chi} h^2 < 0.2$ have been imposed. For details on the computational procedure, see [134, 196]. The filled circles denote higgsino-like models with gaugino fraction $Z_g < 0.01$, squares are mixed models with $0.01 < Z_g < 0.99$ and triangles are gaugino models with $Z_g > 0.99$.

of neutralinos is very efficiently captured by the Earth if $m_{\chi} \lesssim 160$ GeV, and could give an enhanced muon flux by an order of magnitude. This effect is included in Fig. 11. The correspondingly increased scattering rate in direct detectors is not easily detected because of the low recoil energy, but a direction-sensitive detector could be of great help [201].

If a signal were established, one can use the angular spread caused by the radial distribution of neutralinos (in the Earth) and by the energy-dependent mismatch between the direction of the muon and that of the neutrino (for both the Sun and the Earth) to get a rather good estimate of the neutralino mass [199]. If muon energy can also be measured, one can do even better [200].

10. Conclusions and outlook

To conclude, we have seen that the existence of dark matter is more needed than ever, in order to explain a wealth of new observations. In addition to a large density of matter of unknown composition, the universe seems to contain also a large quantity of dark energy, of even more mysterious origin. Since the success of big bang nucleosynthesis combined with the measured intensity of the microwave background greatly constrains the amount of baryonic matter allowed, the major part of the matter density seems to

be of non-baryonic origin.

The standard big bang model contains the required mechanism to create a relic density of electrically neutral, stable particles which, if their interactions are of electroweak strength, may be perfect candidates for dark matter. Foremost of these candidates are the hypothetical supersymmetric partners of electrically neutral ordinary particles, motivated by current thinking in particle physics. Also the more weakly interacting low-mass axions which were invented to solve the strong CP problem are attractive dark matter candidates, probed by sensitive on-going experiments.

Both direct and indirect detection methods have the potential of investigating supersymmetric and similar massive particle dark matter candidates. In particular, a combination of accelerator searches, new solid state, liquid or gas detectors, space-borne gamma-ray and air Cherenkov telescopes as well as neutrino telescopes may have the sensitivity needed to rule out or confirm the supersymmetry solution of the dark matter problem.

Since also the experimental situation concerning massive neutrinos and axions is getting clearer, there is a chance to reach the goal of explaining the nature of the dark matter in the not too distant future.

However, rapid success is by no means guaranteed. It may be that the dark matter problem will plague the scientific community for a long time also in the new millennium. With the realization that dark vacuum energy may be an additional important component of our Universe, the mystery of its inner workings has deepened. However, this is a situation that is likely to inspire a young generation of physicists and astronomers to even more spectacular progress than the remarkable achievements since the 1930's when Zwicky first took notice of the dark matter problem.

Acknowledgments

I wish to thank my collaborators, in particular Joakim Edsjö, Paolo Gondolo and Piero Ullio, for many helpful discussions. Also, I want to thank Elliott Bloom, Sandro Bottino, Jim Buckley, Per Carlson, Thibault Damour, Ulf Danielsson, Nicolao Fornengo, Tom Francke, Tom Gaisser, Ariel Goobar, Per Olof Hulth, Marc Kamionkowski, Lawrence Krauss, Joel Primack, Georg Raffelt, Hector Rubinstein, Pierre Sikivie, Joe Silk, and Michael Turner for useful input to this review.

This work has been supported in part by the Swedish Natural Science Research Council (NFR).

- [1] S. Sarkar, Rep. Prog. Phys. **59** (1996) 1493; D.N. Schramm and M. Turner, Rev. Mod. Phys. **70** (1998) 303; K.A. Olive and D. Thomas, Astropart. Phys. **7** (1997) 27.
- [2] N. Bahcall, J.P. Ostriker, S. Perlmutter and P.J. Steinhardt, Science **284**, 1481 (1999).
- [3] P.J. Steinhardt, L. Wang and I. Zlatev, Phys. Rev. **D59** (1999) 123504.
- [4] S. Perlmutter et al., Astrophys. J. **517** (1999) 565.
- [5] P.M. Garnavich et al., Astrophys. J. **509** (1998) 74.
- [6] L. Bergström and A. Goobar, *Cosmology and Particle Astrophysics*, Wiley/Praxis (Chichester), 1999.

- [7] Y. Fukuda et al., Phys. Rev. Lett. **82** (1998) 2644.
- [8] G. Gelmini and P. Gondolo, Nucl. Phys. **B360** (1991) 145.
- [9] L. Roszkowski, Phys. Rev. **D50** (1994) 4842.
- [10] G. Jungman, M. Kamionkowski and K. Griest, Phys. Rep. **267** (1996) 195.
- [11] G.F. Giudice, I. Tkachev and A. Riotto, Journal of High Energy Physics **9908** (1999) 009.
- [12] A.H. Guth, Phys. Rev. **D23** (1981) 347; A. Linde, Phys. Lett. **B108** (1982) 389; A. Albrecht and P.J. Steinhardt, Phys. Rev. Lett. **48** (1982) 1220.
- [13] S. Weinberg, Rev. Mod. Phys. **61** (1989) 1.
- [14] A.D. Dolgov, Proc. of *Phase Transitions in Cosmology, Fourth Paris Colloquium*, H. J. De Vega and N. Sanchez eds. (1998), 161.
- [15] P.J.E. Peebles, *Principles of Physical Cosmology*, Priceton University Press, 1993.
- [16] C.H. Lineweaver and D. Barbosa, Astrophys. J. **495** (1998) 624; M. Tegmark, Astrophys.J. **514** (1999) L69.
- [17] M. Fukugita, T. Futamase and M. Kasai, Month. Not. Roy. Astr. Soc. **246** (1990) 24P.
- [18] P. Schneider, J. Ehlers and E.E. Falco, *Gravitational Lenses*, Springer-Verlag, 1994.
- [19] E.E. Falco, C.S. Kochanek and J.A. Munoz, Astrophys. J. **494** (1998) 47.
- [20] M. Bartelmann, A. Huss, J.M. Colberg, A. Jenkins and F.R. Pierce, Astron. and Astrophys. **330** (1998) 1.
- [21] J.A. Tyson, G.P. Kochanski and I.P. Dell'Antonio, Astrophys. J. Lett. **498** (1998) 107.
- [22] D.E. Holz and R.M. Wald, Phys. Rev. **D58** (1998) 063501.
- [23] R.B. Metcalf and J. Silk, Astrophys. J. **519** (1999) L1.
- [24] L. Bergström, M. Goliath, A. Goobar and E. Mörtzell, astro-ph/9912194 (1999).
- [25] Y. Sigad, A. Eldar, A. Dekel, M.A. Strauss and A. Yahil, Astrophys. J. **495** (1998) 516.
- [26] B. Chaboyer, P. Demarque, P.J. Kernan and L.M. Krauss, Astrophys. J. **494** (1998) 96.
- [27] M. Kamionkowski and A. Kosowsky, Ann. Rev. Nuc. Part. Sci., 1999.
- [28] The BOOMERANG Collaboration, A. Melchiorri et al., astro-ph/9911445 (1999).
- [29] S. Perlmutter, M. Turner and M. White, Phys. Rev. Lett. **83** (1999) 670.
- [30] R. Bond and A. Szalay, Astrophys. J. **274** (1983) 443.
- [31] E. Gawiser and J. Silk, Science **280** (1998) 1405.
- [32] D.H. Weinberg et al., Astrophys. J. **522** (1999) 563.
- [33] S.L. Bridle et al., astro-ph/9903472 (1999).
- [34] R. Sadat, A. Blanchard and J. Oukbir, Astron. and Astrophys. **329** (1998) 21.
- [35] N. Bahcall and X. Fan, Astrophys. J. **504** (1998) 1.
- [36] A. Kashlinsky, Phys. Rep. **307** (1998) 67.
- [37] R.G. Carlberg et al., Astrophys. J. **516** (1999) 552.
- [38] S.D.M. White et al., Nature **366** (1993) 429.
- [39] A. Songaila, L. Cowie, C. Hogan and M. Rugers, Nature **368** (1994) 599.
- [40] D.Tytler, X.-M. Fan and S. Burles, Nature **381** (1996) 207;
- [41] G.P. Holder and J.E. Carlstrom, astro-ph/9904220 (1999).
- [42] B. Moore, Nature **370** (1994) 629.
- [43] R.A. Flores and J.R. Primack, Astrophys. J. **427** (1994) L1.
- [44] M. Kamionkowski and A.R. Liddle, astro-ph/9911103 (1999).
- [45] D.N. Spergel and P.J. Steinhardt, astro-ph/9909386 (1999).
- [46] F.C. van den Bosch et al., astro-ph/9911372 (1999).
- [47] J.G. Bartlett et al., Science **267** (1995) 980.
- [48] J.H. Oort, Bull. Astron. Inst. Netherlands **15** (1960) 45.
- [49] K. Kuijken and G. Gilmore, Month. Not. Roy. Ast. Soc. **239** (1989) 651.
- [50] K.M. Ashman, Pub. Astr. Soc. Pac. **104** (1992) 1109.
- [51] S.F. Anderson, C.J. Hogan and B.F. Williams, Astron. J. **117** (1999) 56.
- [52] MACHO Collaboration, C. Alcock et al., Proc. of *The Third Stromlo Symposium: The Galactic Halo*, eds. B.K. Gibson, T.S. Axelrod and M.E. Putman, ASP Conference Series **165** (1999)

362.

- [53] B. Paczynski, *Astrophys. J.* **304** (1986) 1.
- [54] MACHO Collaboration, C. Alcock et al., *Nature* **365** (1993) 621.
- [55] EROS Collaboration, E. Aubourg et al., *Nature* **365** (1993) 623.
- [56] MACHO Collaboration, C. Alcock et al., *astro-ph/0001272* (2000).
- [57] D. Zaritsky and D.N.C. Lin, *Astron. J.* **114** (1997) 2545; D. Zaritsky, S.A. Shectman, I. Thompson, J. Harris and D.N.C. Lin, *Astronom. J.* **117** (1999) 2268.
- [58] P. Salati et al., *Astron. and Astrophys.* **350** (1999) 57.
- [59] B.D. Fields, K. Freese and D.S. Graff, *New Astronomy* **3** (1998) 347.
- [60] B.J. Carr and M. Sakellariadou, *Astrophys. J.* **516** (1999) 195.
- [61] S.P. Boughn and J.M. Uson, *Astrophys. J.* **488** (1997) 44.
- [62] D.S. Graff, K. Freese, T.P. Walker and M.H. Pinsonneault, *Astrophys. J.* **523** (1999) L77.
- [63] S. Feltzing, G. Gilmore and R.F.G. Wyse, *Astrophys. J.* **516** (1999) L17.
- [64] P. Ivanov, P. Naselsky and I. Novikov, *Phys. Rev.* **D50** (1994) 7173.
- [65] M. Persic and P. Salucci, *Astrophys. J. Suppl.* **99** (1995) 501.
- [66] J. Binney and W. Dehnen, *Month. Not. Roy. Astr. Soc.* **294** (1998) 429.
- [67] A.V. Kravtsov et al., *Astrophys. J.* **502** (1998) 48.
- [68] L. Bergström, P. Ullio and J.H. Buckley, *Astropart. Phys.* **9** (1998) 137.
- [69] E.I. Gates, G. Gyuk and M.S. Turner, *Astrophys. J. Lett.* **449** L123.
- [70] M. Kamionkowski and A. Kinkhabwala, *Phys. Rev.* **D57** (1998) 3256.
- [71] A. Drukier, K. Freese and D. Spergel, *Phys. Rev.* **D33** (1986) 3495; K. Freese, J. Frieman and A. Gould, *Phys. Rev.* **D37** (1988) 3388.
- [72] G. Gilmore, in *Proc. of International Workshop on the Identification of Dark Matter (IDM 96)*, N.J.C. Spooner (ed.), World Scientific, 1997.
- [73] A. Burkert and J. Silk, *Astrophys. J. Lett.* **488** (1997) 55.
- [74] E. Corbelli and P. Salucci, *astro-ph/9909252* (1999).
- [75] NED image from STScI Digitized Sky Survey, <http://nedwww.ipac.caltech.edu>. The NASA/IPAC Extragalactic Database (NED) is operated by the Jet Propulsion Laboratory, California Institute of Technology, under contract with the National Aeronautics and Space Administration.
- [76] M. Milgrom, *Astrophys. J.* **270** (1983) 365.
- [77] O. Lahav, P.B. Lilje, J.R. Primack and M.J. Rees, *Month. Not. Roy. Astr. Soc.* **251** (1991) 128; L. Bergström and U. Danielsson, *astro-ph/0002152* (2000).
- [78] P. Hut, *Phys. Lett.* **69B** (1977) 85.
- [79] B.W. Lee and S. Weinberg, *Phys. Rev. Lett.* **39** (1977) 165.
- [80] M.I. Vysotsky, A.D. Dolgov and Ya. B. Zel'dovich, *JETP Lett.* **26** (1977) 188.
- [81] J. E. Gunn, B.W. Lee, I. Lerche, D.N. Schramm and G. Steigman, *Astrophys. J.* **223** (1978) 1015.
- [82] K. Griest and M. Kamionkowski, *Phys. Rev. Lett.* **64** (1990) 615.
- [83] D.J.H. Chung, E.W. Kolb and A. Riotto, *Phys. Rev.* **D60** (1999) 063504.
- [84] J. Ellis, J. Lopez and D.V. Nanopoulos, *Phys. Lett.* **B247** (1990) 257; J. Ellis et al., *Nucl. Phys.* **B373** (1992) 399.
- [85] Z.G. Berezhiani and A.D. Dolgov, *Phys. Lett.* **B375** (1996) 26.
- [86] N. Arkani-Hamed, S. Dimopoulos, G. Dvali and N. Kaloper, *hep-ph/9911386* (1999).
- [87] Particle Data Group, C. Caso et al., *Eur. Phys. J.* **C3** (1998) 1.
- [88] C. Athanassopoulos et al., *Phys. Rev. Lett.* **77** (1996) 3082.
- [89] B. Zeitnitz et al., *Prog. Part. Nucl. Phys.* **40** (1998) 169.
- [90] The BooNE Collaboration, E. Church et al., *FERMILAB-PUB-P-0898* (1998).
- [91] J.N. Bahcall et al., *Phys. Rev. Lett.* **78** (1997) 171.
- [92] J. Ellis and S. Lola, *Phys. Lett.* **B458** (1999) 310.
- [93] The Kamiokande Collaboration, K.S. Hirata et al., *Phys. Lett.* **B205** (1988) 416.
- [94] The IMB Collaboration, D. Casper et al., *Phys. Rev. Lett.* **66** (1991) 2561.
- [95] The Soudan-2 Collaboration, W.W.M. Allison et al., *Phys. Lett.* **B449** (1999) 137.

- [96] The MACRO Collaboration, M. Ambrosio et al., Phys. Lett. **B434** (1998) 451.
- [97] W. Hu, D.J. Eisenstein and M. Tegmark, Phys. Rev. Lett. **80** (1998) 5255.
- [98] S. Tremaine and J.G. Gunn, Phys. Rev. Lett. **42** (1979) 407.
- [99] R. Peccei and H.R. Quinn, Phys. Rev. Lett. **38** (1977) 1440.
- [100] S. Weinberg, Phys. Rev. Lett. **40** (1978) 223.
- [101] F. Wilczek, Phys. Rev. Lett. **40** (1978) 279.
- [102] M. Dine, W. Fischler and M. Srednicki, Phys. Lett. **B104** (1981) 199; A.R. Zhitnitsky, Sov. J. Nucl. Phys. **31** (1980) 260.
- [103] J.E. Kim, Phys. Rev. Lett. **43** (1979) 103; M.A. Shifman, A.I. Vainshtein and V.I. Zakharov, Nucl. Phys. **B166** (1980) 493.
- [104] H. Murayama, G. Raffelt, C. Haggmann, K. van Bibber, and L.J. Rosenberg, Eur. Phys. J. **C3** (1998) 264.
- [105] J.E. Kim, Phys. Rev. Lett. **43** (1979) 103; M.A. Shifman, A.I. Vainshtein and V.I. Zakharov, Nucl. Phys. **B166** (1980) 493; M. Dine, W. Fischler and M. Srednicki, Phys. Lett. **104B** (1981) 199.
- [106] G. Raffelt, Nucl. Phys. Proc. Suppl. **77** (1999) 456.
- [107] P. Sikivie, Phys. Rev. Lett. **48** (1982) 1156.
- [108] C. Haggmann et al., Phys. Rev. Lett. **80** (1998) 2043.
- [109] I. Ogawa, S. Matsuki and K. Yamamoto, Phys. Rev. **D53** (1996) 1740.
- [110] P. Fayet, Phys. Lett. **86B** (1979) 272.
- [111] N. Cabibbo, G. Farrar and L. Maiani, Phys. Lett. **105B** (1981) 155.
- [112] H. Pagels and J.R. Primack, Phys. Rev. Lett. **48** (1982) 223.
- [113] S. Weinberg, Phys. Rev. Lett. **50** (1983) 387.
- [114] H. Goldberg, Phys. Rev. Lett. **50** (1983) 1419.
- [115] L.M. Krauss, Nucl. Phys. **B227** (1983) 556.
- [116] J. Ellis, J.S. Hagelin, D.V. Nanopoulos, K. Olive, M. Srednicki, Nucl. Phys. **B238** (1984) 453.
- [117] H.E. Haber and G.L. Kane, Phys. Rep. **117** (1985) 75.
- [118] T. Falk, K.A. Olive and M. Srednicki, Phys. Lett. **B354** (1995) 99; T. Falk, A. Ferstl and K.A. Olive, Phys. Rev. **D59** (1999) 055009; U. Chattopadhyay, T. Ibrahim and P. Nath, Phys. Rev. **D60** (1999) 063505; P. Gondolo and K. Freese, hep-ph/9908390 (1999); S.Y. Choi, hep-ph/9908397 (1999).
- [119] A. Bottino et al., Phys. Lett. **B423** (1998) 109.
- [120] U. Amaldi, W. de Boer and H. Furstenau, Phys. Lett. **B260** (1991) 447.
- [121] See, e.g., J. Polchinski, Rev. Mod. Phys. **68** (1996) 1245; J. Maldacena, Int. J. Theor. Phys. **38** (1999) 1113.
- [122] V. Berezhinsky, A.J. Joshipura and J.F.W. Valle, Phys. Rev. **D57** (1998) 147.
- [123] A. Blondel, Talk at LEPC, November 9, 1999.
- [124] J. Edsjö and P. Gondolo, Phys. Rev. **D56** (1997) 1879.
- [125] V. Berezhinsky et al., Astropart. Phys. **5** (1996) 1.
- [126] J. Ellis, T. Falk and K.A. Olive, Phys. Lett. **B444** (1998) 367; J. Ellis, T. Falk, K.A. Olive and M. Srednicki, hep-ph/9905481 (1999).
- [127] M. Dine, W. Fischler and M. Srednicki, Nucl. Phys. **B189** (1981) 575.
- [128] S. Dimopoulos, G.F. Giudice and A. Pomarol, Phys. Lett. **B389** (1996) 37.
- [129] V. Berezhinsky et al., Astropart. Phys. **5** (1996) 1.
- [130] See, e.g., P. Abreu et al. (DELPHI Collaboration), Phys. Lett. **B446** (1999) 75; J. Ellis, T. Falk and K.A. Olive, Phys. Lett. **B413** (1997) 355.
- [131] P. Nath and R. Arnowitt, Phys. Lett. **B336** (1994) 395.
- [132] F.M. Borzumati, M. Drees and M.M. Nojiri, Phys. Rev. **D51** (1995) 341.
- [133] L. Bergström and P. Gondolo, Astropart. Phys. **5** (1996) 263.
- [134] L. Bergström, T. Damour, J. Edsjö, L. M. Krauss and P. Ullio, JHEP **9908**, (1999) 010.
- [135] L. Bergström, J. Edsjö, P. Gondolo and P. Ullio, Phys. Rev. **D59** (1999) 043506.

- [136] L.J. Hall, T. Moroi and H. Murayama, Phys. Lett. **B424** (1998) 305.
- [137] L. Covi, J.E. Kim and L. Roszkowski, Phys. Rev. Lett. **82** (1999) 4180.
- [138] S.A. Bonometto, F. Gabbiani and A. Masiero, Phys. Rev. **D49** (1994) 3918.
- [139] T. Goto and M. Yamaguchi, Phys. Lett. **B276** (1992) 103.
- [140] A. Kusenko, V. Kuzmin, M. Shaposhnikov and P.G. Tinyakov, Phys. Rev. Lett. **80** (1998) 3185.
- [141] M.W. Goodman and E. Witten, Phys. Rev. **D31** (1985) 3059.
- [142] A. Bottino et al., Phys. Lett. **B402** (1997) 113.
- [143] J. Ellis, R.A. Flores and J.D. Lewin, Phys. Lett. **B212** (1988) 375.
- [144] S. Åminneborg, L. Bergström, and B.-Å. Lindholm, Phys. Rev. **D43(1991)** 2527.
- [145] J. Engel and P. Vogel, hep-ph/9910409 (1999).
- [146] G.D. Starkman and D.N. Spergel, Phys. Rev. Lett. **74** (1995) 2623.
- [147] S.P. Ahlen et al., Phys. Lett. **B195** (1987) 603.
- [148] J. Ellis and R. Flores, Phys. Lett. **B263** (1991) 259.
- [149] J. Engel, Phys. Lett. **B264** (1991) 114.
- [150] M. Drees and M. Nojiri, Phys. Rev. **D48** (1993) 3483.
- [151] D. Bailin, G.V. Kraniotis and A. Love, Nucl. Phys. **B556** (1999) 23.
- [152] Heidelberg-Moscow Collaboration, L. Baudis et al., Phys. Rev. **D59** (1999) 022001; CDMS Collaboration, R.W. Schnee et al., Phys. Rep. **307** (1998) 283; DAMA Collaboration, P. Belli et al., Phys. Rep. **307** (1998) 269; UKDM Collaboration, P. Smith et al., Phys. Rep. **307** (1998) 275.
- [153] A. Bottino, F. Donato, N. Fornengo and S. Scopel, hep-ph/9909228 (1999).
- [154] R. Bernabei et al., Phys. Lett. **B450** (1999) 448.
- [155] A. Bottino, F. Donato, N. Fornengo and S. Scopel, Phys. Lett. **B423** (1998) 109.
- [156] R. Arnowitt and P. Nath, Phys. Rev. **D60** (1999) 044002.
- [157] G. Gerbier, J. Mallet., L. Mosca and C. Tao, astro-ph/9902194 (1999).
- [158] CDMS Collaboration, R. Schnee, talk presented at Inner Space/Outer Space II, Chicago, May 26-29, 1999.
- [159] P. Belli et al., Phys. Rev. **D61** (1999) 023512.
- [160] M. Brhlik and L. Roszkowski, Phys. Lett. **B464** (1999) 303.
- [161] GENIUS Collaboration, L. Baudis et al., hep-ph/9910205 (1999).
- [162] CRESST Collaboration, M. Bravin et al., Astropart. Phys. **12** (1999) 107.
- [163] UKDMC Collaboration, T.J. Sumner et al., Nucl. Phys. Proc. Suppl. **70** (1999) 74.
- [164] D.N. Spergel, Phys. Rev. **D37** (1988) 1353.
- [165] C. Martoff et al., Phys. Rev. Lett. **76** (1996) 4882.
- [166] P. Sikivie, I.I. Tkachev and Y. Wang, Phys. Rev. **D56** (1997) 1863; P. Sikivie, Phys. Lett. **B432** (1998) 139.
- [167] T. Damour and L.M. Krauss, Phys. Rev. Lett. **81** (1998) 5726.
- [168] S.W. Barwick et al., Phys. Rev. Lett. **75** (1995) 390; Astrophys. J. **482** (1997) L191.
- [169] CAPRICE Collaboration, M. Boezio et al., Proc. of the 26th ICRC, contribution OG 1.1.16 (1999), Salt Lake City, USA.
- [170] G. Jungman and M.Kamionkowski, Phys. Rev. **D49** (1994) 2316; A. Bottino, C. Favero, N. Fornengo, G. Mignola, Astropart. Phys. **3** (1995) 77.
- [171] CAPRICE Collaboration, M. Boezio et al., Astrphys. J. **487** (1997) 415.
- [172] BESS Collaboration, A. Moiseev et al., Astrophys. J. **474** (1997) 479.
- [173] S.P. Ahlen et al., Nucl. Instr. Methods **A350** (1994) 351; J. Alcaraz et al., Phys. Lett. **B461** (1999) 387.
- [174] L. Bergström, J. Edsjö and P. Ullio, Astrophys. J. **526** (1999) 215.
- [175] J.W. Bieber et al., Phys. Rev. Lett. **83** (1999) 674.
- [176] E.A. Baltz and P. Gondolo, Phys. Rev. **D57** (1998) 2969.
- [177] P. Ullio, astro-ph/9904086 (1999).
- [178] F. Donato, N. Fornengo and P. Salati, hep-ph/9904481 (1999).

- [179] H.U. Bengtsson, P. Salati and J. Silk, Nucl. Phys. **B346** (1990) 129.
- [180] M. Srednicki, S. Theisen and J. Silk, Phys. Rev. Lett. **56** (1986) 263; *Erratum-ibid* **56** (1986) 1883.
- [181] L. Bergström and H. Snellman, Phys. Rev. **D37**, (1988) 3737.
- [182] A. Bouquet, P. Salati and J. Silk, Phys. Rev. **D40**, (1989) 3168; G. Jungman and M. Kamionkowski, Phys. Rev. **D51** (1995) 3121.
- [183] M. Urban et al., Phys. Lett. **B293** (1992) 149; L. Bergström and J. Kaplan, Astropart. Phys. **2** (1994) 261; P. Ullio and L. Bergström, Phys. Rev. **D57** (1998) 1962.
- [184] S. Rudaz, Phys. Rev. **D39** (1989) 3549.
- [185] L. Bergström and P. Ullio, Nucl. Phys. **B504** (1997) 27; Z. Bern, P. Gondolo and M. Perelstein, Phys. Lett. **B411** (1997) 86.
- [186] S.C. Strausz, Phys. Rev. **D55** (1997) 4566.
- [187] S.D. Biller and J.H. Buckley, Phys. Rev. **D57** (1998) 2637.
- [188] J.F. Navarro, C.S. Frenk and S.D.M. White, Astrophys. J. **462** (1996) 563.
- [189] GLAST Collaboration, A. Moiseev et al., astro-ph/9912139 (1999).
- [190] P. Gondolo and J. Silk, Phys. Rev. Lett. **83** (1999) 1719.
- [191] S. Ritz and D. Seckel, Nucl. Phys. **304** (1988) 877.
- [192] J. Edsjö, Ph.D. Thesis, Uppsala Univ., hep-ph/9504205.
- [193] F. Halzen, Comments Nucl. Part. Phys. **22** (1997) 155.
- [194] A. Bottino, N. Fornengo, G. Mignola and L. Moscoso, Astropart. Phys. **3** (1995) 65; V. Berezhinsky et al., Astropart. Phys. **5** (1996) 333.
- [195] L. Bergström, J. Edsjö and P. Gondolo, Phys. Rev. **D55** (1997) 1765.
- [196] L. Bergström, J. Edsjö and P. Gondolo, Phys. Rev. **D58** (1998) 103519.
- [197] T.K. Gaisser, F. Halzen and T. Stanev, Phys. Rep. **258** (1995) 173.
- [198] M. Kamionkowski, G. Jungman, K. Griest and B. Sadoulet, Phys. Rev. Lett. **74** (1995) 5174.
- [199] J. Edsjö and P. Gondolo, Phys. Lett. **B357** (1995) 595.
- [200] L. Bergström, J. Edsjö and M. Kamionkowski, Astropart. Phys. **7** (1997) 147.
- [201] T. Damour and L.M. Krauss, Phys. Rev. **D59** (1999) 063509.